# NMR and EPR Studies of the Bis(pyridine) and Bis( tert -butyl isocyanide) Complexes of Iron(III) Octaethylchlorin

**ARTICLE** *in* INORGANIC CHEMISTRY · APRIL 2005

Impact Factor: 4.76 · DOI: 10.1021/ic0490876 · Source: PubMed



**3 AUTHORS**, INCLUDING:

Sheng Cai
Technische Universität Dortmund
**17** PUBLICATIONS **345** CITATIONS
SEE PROFILE

F(rances) Ann Walker
The University of Arizona
**242** PUBLICATIONS **8,709** CITATIONS
SEE PROFILE

*Inorg. Chem.* **2005**, *44*, 1890–1903


# NMR and EPR Studies of the Bis(pyridine) and Bis(*tert*-butyl isocyanide) Complexes of Iron(III) Octaethylchlorin

**Sheng Cai, Dennis L. Lichtenberger,* and F. Ann Walker***

*Department of Chemistry, University of Arizona, Tucson, Arizona 85721-0041*

Received July 9, 2004

The NMR and EPR spectra of a series of pyridine complexes $[(OEC)Fe(L)_2]^+$ (L = 4-$Me_2$NPy, Py, and 4-CNPy) have been investigated. The EPR spectra at 4.2 K suggest that, with a decrease of the donor strength of the axial ligands, the complexes change their ground state from $(d_{xy})^2(d_{xz}d_{yz})^3$ to $(d_{xz}d_{yz})^4(d_{xy})^1$. The NMR data from 303 to 183 K show that at any temperature within this range the chemical shifts of pyrrole-8,17-$CH_2$ protons increase with a decrease in the donor strength of the axial ligands. The full peak assignments of the $[(OEC)Fe(L)_2]^+$ complexes of this study have been made from COSY and NOE difference experiments. The pyrrole-8,17-$CH_2$ and pyrroline protons show large chemical shifts (hence indicating large $\pi$ spin density on the adjacent carbons which are part of the $\pi$ system), while pyrrole-12,13-$CH_2$ and -7,18-$CH_2$ protons show much smaller chemical shifts, as predicted by the spin densities obtained from molecular orbital calculations, both Hückel and DFT; the DFT calculations additionally show close energy spacing of the highest five filled orbitals (of the Fe(II) complex) and strong mixing of metal and chlorin character in these orbitals that is sensitive to the donor strength of the axial substituents. The pattern of chemical shifts of the pyrrole-$CH_2$ protons of $[(OEC)Fe(t\text{-BuNC})_2]^+$ looks somewhat like that of $[(OEC)Fe(4\text{-}Me_2NPy)_2]^+$, while the chemical shifts of the *meso*-protons are qualitatively similar to those of $[(OEP)Fe(t\text{-BuNC})_2]^+$. The temperature dependence of the chemical shifts of $[(OEC)Fe(t\text{-BuNC})_2]^+$ shows that it has a mixed $(d_{xz}d_{yz})^4(d_{xy})^1$ and $(d_{xy})^2(d_{xz},d_{yz})^3$ electron configuration that cannot be resolved by temperature-dependent fitting of the proton chemical shifts, with a $S = 5/2$ excited state that lies somewhat more than $2kT$ at room temperature above the ground state; the observed pattern of chemical shifts is the approximate average of those expected for the two $S = 1/2$ electronic configurations, which involve the *a*-symmetry SOMO of a planar chlorin ring with the unpaired electron predominantly in the $d_{yz}$ orbital and the *b*-symmetry SOMO of a ruffled chlorin ring with the unpaired electron predominantly in the $d_{xy}$ orbital. A rapid interconversion between the two, with calculated vibrational frequency of 22 $cm^{-1}$, explains the observed pattern of chemical shifts, while a favoring of the ruffled conformation explains the negative chemical shift (and thus the negative spin density at the $\alpha$-pyrroline ring carbons), of the pyrroline-H of $[TPCFe(t\text{-BuNC})_2]CF_3SO_3$ (Simonneaux, G.; Kobeissi, M. *J. Chem. Soc., Dalton Trans.* **2001**, 1587–1592). Peak assignments for high-spin (OEC)FeCl have been made by saturation transfer techniques that depend on chemical exchange between this complex and its bis-4-$Me_2$NPy adduct. The contact shifts of the pyrrole-$CH_2$ and *meso* protons of the high-spin complex depend on both $\sigma$ and $\pi$ spin delocalization due to contributions from three of the occupied frontier orbitals of the chlorin ring.

## Introduction

Among the "green" hemes that catalyze biological reactions are the heme *d* of the cytochrome *bd* terminal oxidase of *Escherichia coli*,[1−4] the heme *d* of the catalase HPII from *E. coli*,[5−7] and the sulfhemes.[8,9] All of these pigments are iron chlorin complexes which have uniquely different

* Authors to whom correspondence should be addressed. E-mail: awalker@u.arizona.edu (F.A.W.); dlichten@u.arizona.edu (D.L.L.).

(1) Jünemann, S., *Biochim. Biophys. Acta* **1997**, *1321*, 107−127.
(2) Jasaitis, A.; Borisov, V. B.; Belevich, N. P.; Morgan, J. E.; Konstantinov, A. A.; Verhovsky, M. I. *Biochemistry* **2000**, *39*, 13800−13809.
(3) Lorence, R. M.; Koland, J. G.; Gennis, R. B. *Biochemistry* **1986**, *25*, 2314−2321.
(4) Sotiriou, C.; Chang, C. K. *J. Am. Chem. Soc.* **1988**, *110*, 2264−2270.
(5) Bravo, J.; Mate, M. J.; Schneider, T.; Switala, J.; Wilson, K.; Loewen, P. C.; Fita, I. *Proteins: Struct., Funct., Genet.* **1999**, *34*, 155−166.
(6) Loewen, P. *Gene* **1996**, *179*, 39−44.
(7) Chiu, J. T.; Loewen, P. C.; Switala, J.; Gennis, R. B.; Timkovich, R. *J. Am. Chem. Soc.* **1989**, *111*, 7046−7050.



10.1021/ic0490876 CCC: $30.25 
Published on Web 02/25/2005

structures. There has previously been some confusion regarding the classification of reduced hemes and expectations as to their electronic properties, and a number of careful structural investigations were required to elucidate the geometric and stereoisomerism of these macrocycles,[1−9] as well as the "other" green hemes, including heme $d_1$ (a dioxoisobacteriochlorin[10]) and siroheme (an isobacteriochlorin[11,12]).

There have been a number of previous studies of iron chlorin and/or isobacteriochlorin complexes by magnetic resonance techniques, including the seminal paper of Stolzenberg, Strauss, and Holm in 1981[13] and additional papers from these authors,[14−18] as well as other researchers,[19−26] but only one of them has involved investigation of the NMR spectra of the iron(III) bis(imidazole) or (-pyridine) complexes, and the chemical shifts reported for the bis(imidazole) complex of that naturally derived chlorin[19] are somewhat different from those reported herein.

Understanding the electronic properties of the iron(III) complexes of each of the individual "green" hemes is an important step in understanding their mechanisms of action. Hence, we have investigated three bis(pyridine) and the bis(*tert*-butyl isocyanide) complexes of iron(III) *trans*-octaethylchlorin (OEC), Chart 1, as models of hemes *d*. The NMR and EPR spectra of the octaethylchlorin (OEC) complexes are compared to those of the corresponding complexes of octaethylporphyrin (OEP), the bis(imidazole) complexes of (octaethylchlorinato)iron(III) and (oxooctaethylchlorinato)-iron(III) (oxo-OEC)[27] as well as (pyropheophorbide)iron(III) (Ppheo),[19] and a number of bis(ligand) complexes of (tetraphenylchlorinato)iron(III) (TPC)[24−26,38] and of substituted (tetraphenylporphyrinato)iron(III) (TPP, TMP, and others).[39−41] By comparing and contrasting the electronic properties of these molecules with those of the others, this work provides additional information on the factors that control the electronic properties of all of these systems.

**Chart 1**

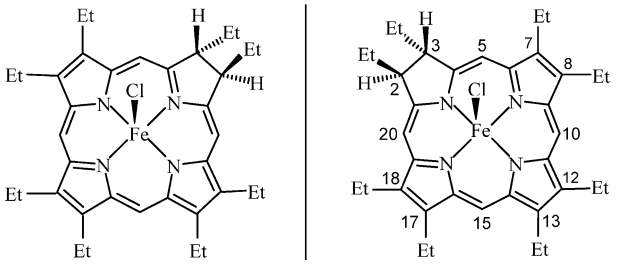


## Experimental Section

**Materials and Sample Preparation.** The (*trans*-octaethylchlorinato)iron(III) chloride, (OEC)FeCl, was synthesized as described previously.[13,18] Deuterated chemicals, pyridine-$d_5$ (D, 99.5%) and methylene-$d_2$ chloride (D, 99.5%), were purchased from Cambridge Isotope Laboratories, and nondeuterated chemicals, 4-(dimethylamino)pyridine, 4-cyanopyridine, and *tert*-butyl isocyanide from Aldrich. Approximately 5 mM (octaethylchlorinato)iron(III) samples

(8) Berzofsky, J. A.; Peisach, J.; Horecker, B. L. *J. Biol. Chem.* **1972**, *247*, 3783−3791.
(9) Chatfield, M. J.; La Mar, G. N.; Kauten, R. J. *Biochemistry* **1987**, *26*, 6939−6950.
(10) Chang, C. K.; Wu, W. *J. Biol. Chem.* **1986**, *261*, 8593−8596.
(11) Crane, B. R.; Siegel, L. M.; Getzoff, E. D. *Biochemistry* **1997**, *36*, 12101−12119.
(12) Stroupe, M. E.; Leech, H. K.; Daniels, D. S.; Warren, M. J.; Getzoff, E. D. *Nat. Struct. Biol.* **2003**, *10*, 1064−1073.
(13) Stolzenberg, A. M.; Strauss, S. H.; Holm, R. H. *J. Am. Chem. Soc.* **1981**, *103*, 4763−4778.
(14) Strauss, S. H.; Pawlik, M. J. *Inorg. Chem.* **1986**, *25*, 1921−1923.
(15) Dixon, D. W.; Woehler, S.; Hong, X.; Stolzenberg, A. M. *Inorg. Chem.* **1988**, *27*, 3682−3685.
(16) Pawlik, M. J.; Miller, P. K.; Sullivan, E. P.; Levstik, M. A.; Almond, D. A.; Strauss, S. H. *J. Am. Chem. Soc.* **1988**, *110*, 3007−3012.
(17) Sullivan, E. P., Jr.; Grantham, J. D.; Thomas, C. S.; Strauss, S. H. *J. Am. Chem. Soc.* **1991**, *113*, 5264−5270.
(18) Holm, R. H.; Kennepohl, P.; Solomon, E. I. *Chem. Rev.* **1996**, *96*, 2239−2314.
(19) Licoccia, S.; Chatfield, M. J.; La Mar, G. N.; Smith, K. M.; Mansfield, K. E.; Anderson, R. R. *J. Am. Chem. Soc.* **1989**, *111*, 6087−6093.
(20) Ozawa, S.; Watanabe, Y.; Morishima, I. *Inorg. Chem.* **1992**, *31*, 4042−4043.
(21) Ozawa, S.; Watanabe, Y.; Morishima, I. *Inorg. Chem.* **1994**, *33*, 306−313.
(22) Ozawa, S.; Watanabe, Y.; Nakashima, S.; Kitagawa, T.; Morishima, I. *J. Am. Chem. Soc.* **1994**, *116*, 634−641.
(23) Ozawa, S.; Watanabe, Y.; Morishima, I. *J. Am. Chem. Soc.* **1994**, *116*, 5832−5838.
(24) Kobeissi, M.; Toupet, L.; Simonneaux, G. *Inorg. Chem.* **2001**, *40*, 4494−4499.
(25) Simonneaux, G.; Kobeissi, M. *J. Chem. Soc., Dalton Trans.* **2001**, 1587−1592.
(26) Simonneaux, G.; Kobeissi, M.; Toupet, L. *Inorg. Chem.* **2003**, *42*, 1644−1651.
(27) Cai, S.; Belikova, E.; Yatsunyk, L. A.; Stolzenberg, A. M.; Walker, F. A. *Inorg. Chem.* **2005**, *44*, 1882−1889.
(28) http://www.shokhirev.com/nikolai/programs/prgsciedu.html.
(29) Frisch, M. J.; Trucks, G. W.; Schlegel, H. B.; Scuseria, G. E.; Robb, M. A.; Cheeseman, J. R.; Montgomery, J. A., Jr.; Vreven, T.; Kudin, K. N.; Burant, J. C.; Millam, J. M.; Iyengar, S. S.; Tomasi, J.; Barone, V.; Mennucci, B.; Cossi, M.; Scalmani, G.; Rega, N.; Petersson, G. A.; Nakatsuji, H.; Hada, M.; Ehara, M.; Toyota, K.; Fukuda, R.; Hasegawa, J.; Ishida, M.; Nakajima, T.; Honda, Y.; Kitao, O.; Nakai, H.; Klene, M.; Li, X.; Knox, J. E.; Hratchian, H. P.; Cross, J. B.; Bakken, V.; Adamo, C.; Jaramillo, J.; Gomperts, R.; Stratmann, R. E.; Yazyev, O.; Austin, A. J.; Cammi, R.; Pomelli, C.; Ochterski, J. W.; Ayala, P. Y.; Morokuma, K.; Voth, G. A.; Salvador, P.; Dannenberg, J. J.; Zakrzewski, V. G.; Dapprich, S.; Daniels, A. D.; Strain, M. C.; Farkas, O.; Malick, D. K.; Rabuck, A. D.; Raghavachari, K.; Foresman, J. B.; Ortiz, J. V.; Cui, Q.; Baboul, A. G.; Clifford, S.; Cioslowski, J.; Stefanov, B. B.; Liu, G.; Liashenko, A.; Piskorz, P.; Komaromi, I.; Martin, R. L.; Fox, D. J.; Keith, T.; Al-Laham, M. A.; Peng, C. Y.; Nanayakkara, A.; Challacombe, M.; Gill, P. M. W.; Johnson, B.; Chen, W.; Wong, M. W.; Gonzalez, C.; Pople, J. A. *Gaussian 03*, revision C.02; Gaussian, Inc.: Wallingford, CT, 2004.
(30) te Velde, G.; Bickelhaupt, F. M.; van Gisbergen, S. J. A.; Fonseca Guerra, C.; Baerends, E. J.; Snijders, J. G.; Ziegler, T. *J. Comput. Chem.* **2001**, *22*, 931−967.
(31) Fonseca Guerra, C.; Snijders, J. G.; te Velde, G.; Baerends, E. J. *Theor. Chem. Acc.* **1998**, *99*, 391.
(32) *ADF2004.01*; SCM, Theoretical Chemistry, Vrije Universiteit: Amsterdam, The Netherlands; http://www.scm.com.
(33) Amashukeli, X.; Gruhn, N. E.; Lichtgenberger, D. L.; Winkler, J. R.; Gray, H. B. *J. Am. Chem. Soc.* **2004**, *126*, 0000−0000.
(34) Flükiger, P. F. Development of the molecular graphics package MOLEKEL and its application to selected problems in organic and organometallic chemistry. Thesis No. 2561, Département de chimie physique, Université de Genève, Geneve, 1992.
(35) Portmann, S.; Lüthi, H. P. MOLEKEL: An Interactive Molecular Graphics Tool. *CHIMIA* **2000**, *54*, 766−770; http://www.cscs.ch/molekel/.
(36) La Mar, G. N.; Walker, F. A. In *The Porphyrins*; Dolphin, D., Ed.; Academic Press: New York, 1979; Vol. IV, pp 61−157.
(37) Walker, F. A. In *The Porphyrin Handbook*; Kadish, K. M., Smith, K. M., Guilard, R., Eds.; Academic Press: San Diego, CA; 2000; Chapter 36, Vol. 5, pp 81−183.
(38) Cai, S.; Shokhireva, T. Kh.; Walker, F. A. To be submitted for publication.
(39) La Mar, G. N.; Gaudio, J. D.; Frye, J. S. *Biochim. Biophys. Acta* **1977**, *498*, 422−435.
(40) Watson, C. T. Ph.D. Dissertation, University of Arizona, 1996.
(41) Watson, C. T.; Cai, S.; Walker, F. A. To be submitted for publication.

for NMR studies were prepared in 5 mm NMR tubes with deuterated methylene chloride as solvent. Complexes with axial ligands were made by directly adding an excess of the desired axial ligand (iron chlorin:axial ligand 1:4 in moles, or ~20 mM axial ligand). For complexes with pyridine and 4-cyanopyridine as axial ligands, an excess of silver trifluoromethanesulfonate ($AgOSO_2CF_3$, 99%, Alfa) was added and the solution filtered prior to addition of the axial ligands to remove chloride. To prevent oxidation of chlorin to porphyrin, $[(OEC)Fe(t\text{-}BuNC)_2]^+$ was prepared in an inert-atmosphere bag. An excess of $AgOSO_2CF_3$ was added to the $CD_2Cl_2$ solution of (OEC)FeCl in an NMR tube, and the tube was shaken to remove the chloride ion as AgCl. Then the solution was filtered into another NMR tube through glass wool and an excess of *t*-BuNC was added. All samples were degassed three times with nitrogen before sealing the NMR tubes.

**NMR Spectroscopy.** For NMR measurements at low temperature, the spectra were recorded on a Varian Unity-300 spectrometer operating at 299.955 MHz with a variable-temperature unit (temperature range from −85 to +30 °C), referenced by the resonance from residual solvent protons (5.32 ppm relative to TMS). The temperature was calibrated using the standard Wilmad methanol and ethylene glycol samples. For other experiments, the spectra were acquired on a Unity-300, Bruker DRX-500, or DRX-600 NMR spectrometer. The 1D saturation transfer or NOE difference experiments were carried out on a DRX-500 or DRX-600 spectrometer using the normal NOE difference pulse sequence. A selective intermediate level pulse (40−45 dB; −6 dB is the maximum) was irradiated on the specific peaks of the fast-relaxing (high-spin) species with an irradiation time of 50 ms, followed by a detection pulse (90°).

**EPR Spectroscopy.** The low-spin bis(ligand) complexes of $(OEC)Fe^{III}$ were prepared in dry $CD_2Cl_2$ immediately before the experiments using the same method as for NMR studies and frozen in liquid nitrogen. The EPR spectra were obtained on a CW EPR spectrometer ESP-300E (Bruker) operating at X-band using 0.2 mW microwave power and 100 kHz modulation amplitude of 2 G. A Systron-Donner microwave counter was used for frequency calibration. The EPR measurements were performed at 4.2 K using an Oxford continuous-flow cryostat, ESR 900.

**Electronic Structure Calculations.** A variety of electronic structure calculations were carried out as an initial exploration of the factors contributing to the electronic states and properties of these molecules. Many of the essential orbital features are apparent from a Hückel analysis of the interaction of the chlorin $\pi$ orbitals with the metal d orbitals using the program MPORPHw.[28] Density functional calculations using both GAUSSIAN03[29] (B3LYP functional) and Amsterdam Density Functional (ADF 2004.01)[30−32] (BLYP functional) approaches were utilized to gain additional insight into the relative orbital energetics and spin density characteristics. Double-$\zeta$ level (6-31G for C, N, and H; LANL2DZ for Fe) and triple-$\zeta$ level (6-311G for C, N, and H; CEP-121G for Fe) GAUSSIAN calculations were compared, and the results were found to be very similar. Only the triple-$\zeta$ level basis calculations are reported for the GAUSSIAN calculations. Polarization functions were added to the triple-$\zeta$ basis for the ADF calculations (standard TZP basis in the ADF package). As an initial model for examining the orbital interactions, idealized structures were constructed in which the pyrrole and pyrroline rings were constrained to the same plane, and the peripheral ethyl substituents of octaethylchlorin were modeled with methyl groups. The methyl groups were held to $C_{3v}$ local symmetry with typical geometric parameters obtained from other optimizations (CH distance of 1.086 Å and CCH angle of 111°), and the methyl groups were not allowed to rotate. A frequency calculation was carried out with the GAUSSIAN program on $[(OMC)Fe(MeNC)_2]$ (OMC = octamethylchlorin), and the only imaginary frequencies were associated with the methyl group orientations. Low vibrational frequencies were found for normal modes associated with ruffling (22 $cm^{-1}$) and saddling (17 $cm^{-1}$)

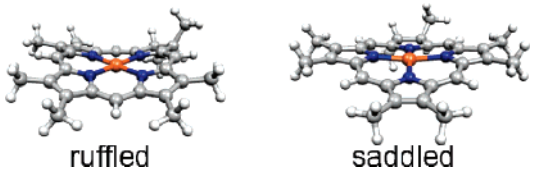


of the chlorin ring, and calculations with these distortions also were investigated. For the ruffled structure, the methylene carbons were placed alternately 0.5 Å above and below the mean chlorin plane, and the twist of the planar pyrrole and pyrroline rings was optimized along with the rest of the structure as described above, according to the distorted positions of the methylene groups. For the saddled structure the planar pyrrole and pyrroline rings are alternately angled up and down from the metal center by 5°, which places the nitrogen atoms ~0.18 Å above and below the mean plane, and the remaining structure was again optimized as above. For $[(OMC)Fe(MeNC)_2]$ the ruffle-distorted structure is calculated to be 4.5 kcal/mol above the planar structure and the saddle-distorted structure is calculated to be 7.5 kcal/mol above the planar structure. For calculations on the $[(OMC)Fe(ImH)_2]$ molecule the imidazoles were aligned in parallel planes that bisect the $C_2-C_3$ bond of the pyrroline ring and the $C_{12}-C_{13}$ bond of the opposite pyrrole ring. All reported geometry optimizations and the frequency calculation are for the neutral molecules with closed-shell singlet electron configurations to examine the orbital descriptions before the consequences of unpaired spin. A geometry optimization of the first positive ion state of the $[(OMC)Fe(ImH)_2]$ molecule (unrestricted doublet state) showed very little change in structure from the neutral molecule, similar to the small reorganization energies with ionization found for metalloporphyrins.[33] For the spin density calculations of the cation molecules, the doublet states were calculated in the unrestricted formalism using the optimized geometries of the neutral molecules. Orbital and density displays are created with the program MOLEKEL.[34,35] Orbital surfaces are displayed with a surface value of 0.03, and spin density surfaces are displayed with a surface value of 0.001.

The optimized structures obtained from the GAUSSIAN and ADF calculations are very similar. For example, geometry optimization of the $[(OMC)Fe(MeNC)_2]$ molecule by ADF starting from the GAUSSIAN coordinates converged in four cycles and the largest change in Fe−N distance was 0.02 Å. Both methods obtain the same occupied molecular orbitals for the neutral molecules, and both place the top five occupied molecular orbitals very close in energy. For $[(OMC)Fe(HIm)_2]$ the GAUSSIAN calculation places the top five occupied orbitals within 0.5 eV and the ADF calculation places them within 1 eV. For $[(OMC)Fe(MeNC)_2]$ the GAUSSIAN calculation places the top five occupied orbitals within 1 eV and the ADF calculation places them within 0.4 eV. The top five orbitals are mixtures of metal d and chlorin $\pi$ character. Due to the small overlap and close energy match between the metal d and chlorin $\pi$ orbitals, the partitioning of metal and chlorin character within the final molecular orbitals is very sensitive to the initial relative energies of the metal d and chlorin $\pi$ orbitals. The ADF calculations tend to place the metal d orbitals slightly less stable relative to the chlorin $\pi$ orbitals than the GAUSSIAN calculations, and thus the ADF calculations place more metal character in the higher occupied orbitals. Given the sensitivity of the orbital characters to these

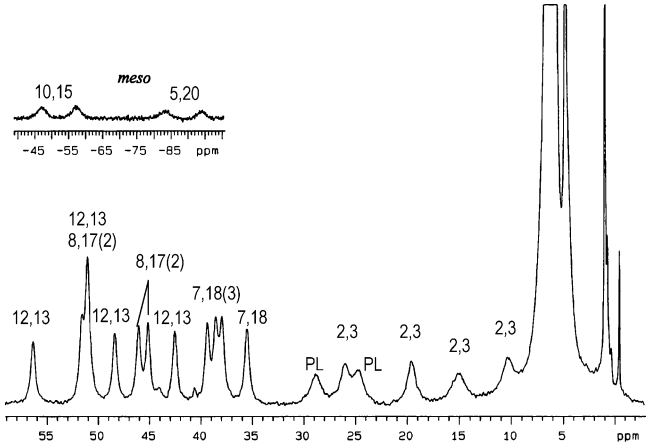


**Figure 1.** $^1$H spectrum of high-spin (OEC)FeCl in $CD_2Cl_2$ at 25 °C. Insert: Region of the four *meso* protons.

methods and the approximations of structure, lack of solvent effects, etc., calculations at this level of theory and modeling cannot confidently determine the spin states of the molecular ions. More detailed theoretical investigation is called for. Nonetheless, the orbital interactions and spin densities obtained for different electronic states provide a framework for interpretation of the experimental data of this study.

## Results and Discussion

**Bis(pyridine) Complexes of (OEC)Fe$^{III}$.** Figure 1 shows the 1D $^1$H NMR spectrum of the high-spin (OEC)FeCl, to be discussed in detail below. As is clear from this spectrum, the molecule has low symmetry (Chart 1) which leads to almost the maximum number of $CH_2$ resonances, 13 of the possible 16, whose assignments will be discussed below. Upon addition of pyridine ligands, the color of the solution changed to green as the bis(ligand) Fe(III) complexes were formed; the $^1$H NMR spectra following addition of 4-$Me_2$-NPy, Py-$d_5$, and 4-CNPy are shown in Figure 2a−c, respectively. The full peak assignments of the bis(ligand) complexes were made from COSY, NOESY, and NOE difference experiments. The peak assignments of the bis-(imidazole-$d_4$) complex of (OEC)Fe$^{III}$ have been reported in the accompanying paper, along with those of [(oxo-OEC)-Fe(Im-$d_4$)$_2$]Cl.[27] Here in the text, except for the 1D spectra, only detailed spectra of [(OEC)Fe(4-$Me_2$NPy)$_2$]Cl and [(OEC)Fe(t-BuNC)$_2$]$SO_3CF_3$ are shown as examples. COSY, NOESY, and/or NOE difference spectra of the other complexes (bis-Py, bis-4-CNPy) are provided in the Supporting Information.

The [(OEC)Fe(4-$Me_2$NPy)$_2$]Cl complex has two kinds of *meso* protons and four kinds of ethyl groups, since it has $C_2$ symmetry along the axis that passes from the center of the pyrroline-2,3 bond to the center of the pyrrole-12,13 bond, Chart 1, with two like axial ligands. For each ethyl group, the two $CH_2$ protons are not equivalent due to the trans configuration of the two pyrroline protons, Chart 1. Thus, a total of eight resonances from $CH_2$ protons and two resonances from the *meso* protons were observed in the NMR spectra of the low-spin complexes. Partial assignments of the $^1$H NMR spectrum of [(OEC)Fe(4-$Me_2$NPy)$_2$]Cl can be made from COSY (Supporting Information Figure S1) and

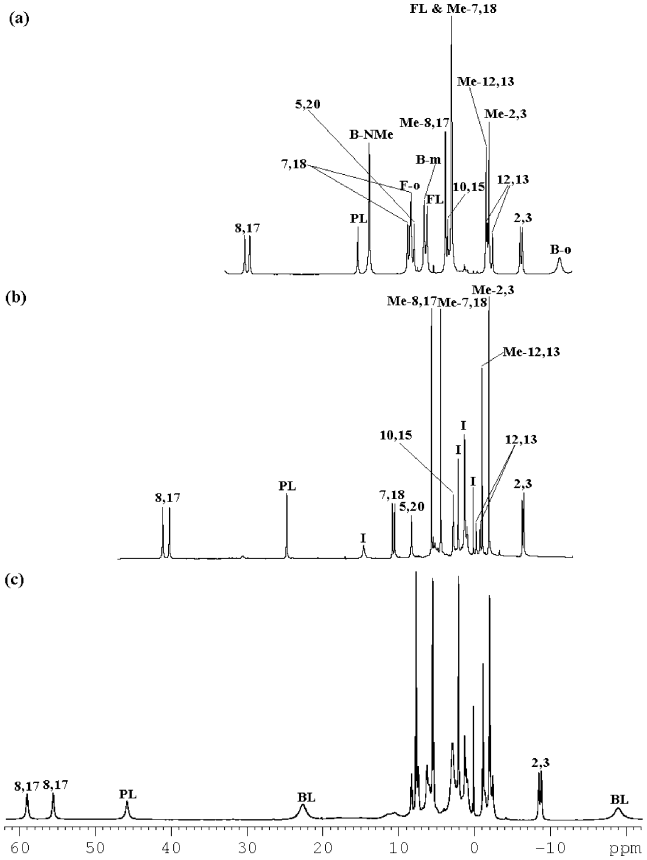


**Figure 2.** (a) $^1$H spectrum of [(OEC)Fe(4-$Me_2$NPy)$_2$]Cl in $CD_2Cl_2$ at 30 °C. (b) $^1$H spectrum of [(OEC)Fe(Py-$d_5$)$_2$]$^+$ in $CD_2Cl_2$ at 30 °C. (c) $^1$H spectrum of [(OEC)Fe(4-CNPy)$_2$]$^+$ in $CD_2Cl_2$ at −20 °C. Key: Me = methyl of the pyrrole ethyl group; PL = pyrroline protons; B or BL = bound axial ligand; FL = free axial ligand; *m* = *meta* proton of the bound ligand; *o* = *ortho* proton of the bound ligand; I = impurity; numbers indicate the positions of the $CH_2$ groups and *meso* protons (Chart 1).

NOESY (Figure S2) experiments. In the COSY spectrum, for each ethyl group there are three pairs of cross-peaks, one between the two different $CH_2$ protons within the ethyl group and one each between the two kinds of $CH_2$ protons and the methyl group. For the pyrroline-2,3 ethyl groups, extra cross-peaks between the $CH_2$ protons and the pyrroline protons were also observed. The two resonances around −6 ppm can be assigned to the pyrroline-2,3-$CH_2$ protons because of the extra cross-peaks connecting the $CH_2$ and pyrroline-H resonances (Figure S1). Consistent with this assignment is the fact that, for pyrrole-$CH_2$ protons, the contact shift from the $\pi$ (as well as $\sigma$) spin delocalization should be always positive.[36,37] The negative sign of the chemical shift of the resonances at −6 ppm must result from the sum of a negative pseudocontact (electron−nuclear dipolar) shift[36,37] and small positive contact and diamagnetic shifts. This assignment is further supported by the NOE difference experiments shown below. The assignments of the axial ligand resonances were made from NOESY/EXSY experiments (Figure S2), where only chemical exchange cross-peaks are observed, between coordinated and free ligand protons, and NOEs are too weak to be observed.

The full assignment of the $CH_2$ groups and *meso* protons of [(OEC)Fe(4-$Me_2$NPy)$_2$]$^+$ was made from NOE difference experiments (Figure 3). Note that only those positive

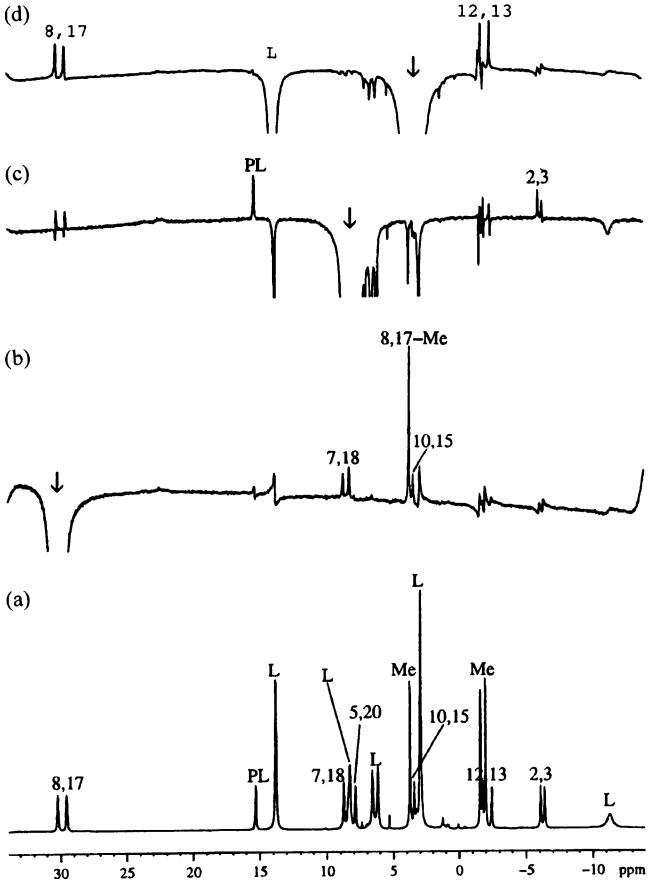


**Figure 3.** NOE difference spectra of $[(OEC)Fe(4\text{-}Me_2NPy)_2]Cl$ at 30 °C: (a) control spectrum; (b−d) difference spectra, where the arrows show the position of irradiation in each case. The negative peak marked with "L" in (d) is the N−Me group of the bound axial ligands, which arises from the chemical exchange between the free and bound axial ligand and is due to the closeness of the N−Me resonance of the free ligand to the resonance being irradiated (*meso*-10,15) and, thus, its partial saturation.

absorptive-phase peaks with a line width larger than 30 Hz are NOE signals; the sharp peaks, which are due to diamagnetic impurities, and those peaks with dispersive shape are artifacts. In Figure 3b, one peak of the doublet at 30 ppm (pyrrole-$CH_2$) was irradiated, resulting in two weak (about 0.1%) NOE signals, one between the peak irradiated and its adjacent $CH_2$ group at 8.5 ppm and the other one between it and its adjacent *meso* proton at 3.5 ppm. (Irradiation of the other peak, which is not shown in this figure, gave the same result.) In addition, much stronger peaks due to a NOE between the two pyrrole-$CH_2$ protons and their $CH_3$ partner resonance at 3.5 ppm are also observed. According to the structure of the chlorin ring, Chart 1, but with two axial ligands, these two adjacent $CH_2$ should be on the $\beta$-pyrrole positions 7,18 or 8,17, although the absolute positional assignments are not defined by this experiment.

In Figure 3c, by irradiation of the other *meso* resonance, at 8 ppm, NOE signals from the pyrroline-2,3-$CH_2$ and the pyrroline-2,3-H are observed. Thus, this peak must be due to the *meso*-5,20 protons. The NOEs between *meso*-5,20 and pyrrole-7,18-$CH_2$ protons are obscured by the large envelope of peaks being irradiated and are thus invisible.

When the other *meso* (*meso*-10,15) proton peak is irradiated (Figure 3d), two NOE signals are observed, one from

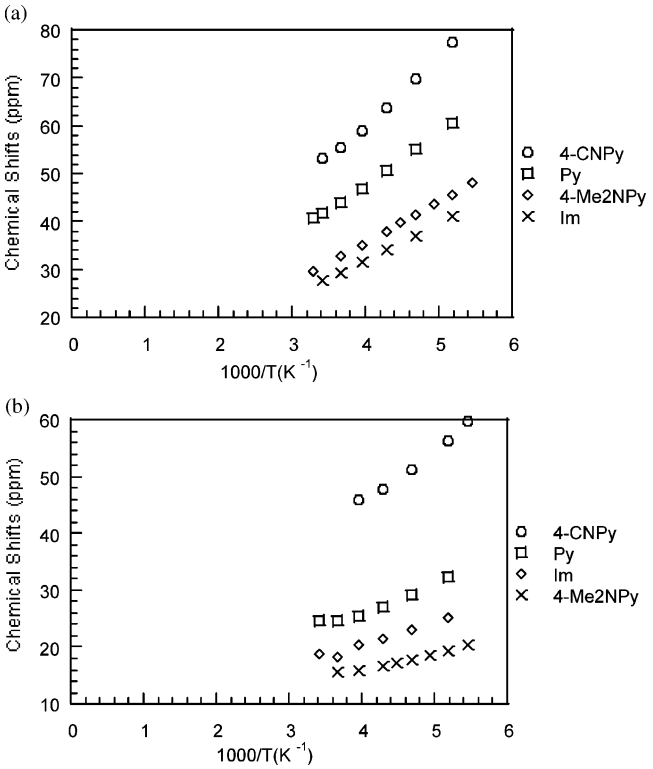


**Figure 4.** (a) Curie plots of the pyrrole-8,17-$CH_2$ proton chemical shifts of the complexes $[(OEC)Fe(L)_2]^+$ (L = Im-$d_4$, 4-$Me_2$NPy, Py, and 4-CNPy). (b) Curie plots of the pyrroline proton chemical shifts of the complexes $[(OEC)Fe(L)_2]^+$ (L = Im-$d_4$, 4-$Me_2$NPy, Py, and 4-CNPy).

pyrrole-8,17-$CH_2$ and the other one from pyrrole-12,13-$CH_2$. According to the results shown in Figure 3b, the doublet at 30 ppm should thus be assigned to pyrrole-8,17-$CH_2$. By this means, pyrrole-12,13-$CH_2$ and pyrrole-7,18-$CH_2$ could also be assigned. In the same way, full assignments for the bis(imidazole)[27] and other bis(pyridine) (Supporting Information Figures S3−S6) complexes of $(OEC)Fe^{III}$ were also made. Curie plots of the 8,17 and pyrroline-$CH_2$ resonances of the bis(imidazole)[27] and the three bis(pyridine) complexes of (OEC)Fe(III) are shown in Figure 4a,b, respectively.

The chemical shifts, their spread, and their temperature dependences for $[(OEC)Fe(4\text{-}Me_2NPy)_2]Cl$ indicate that it is a low-spin Fe(III) complex with a $(d_{xy})^2(d_{xz}d_{yz})^3$ ground state; the small observed *meso*-H shifts are particularly diagnostic of this electronic ground state:[27,37] The chemical shifts of the two kinds of *meso* protons fall in the diamagnetic region, indicating that there is little spin density on the *meso* positions (pseudocontact shifts should be small and negative, as mentioned above). As shown elsewhere for $[(OEC)Fe(Im\text{-}d_4)_2]Cl$[27] and $[(TPC)Fe(HIm)_2]Cl$,[38] $[(OEC)Fe(4\text{-}Me_2NPy)_2]Cl$ also has large spin density on the pyrrole-8,17 and pyrroline-H positions and small spin density on the pyrrole-12,13 and pyrrole-7,18 positions. The NMR spectra of the bis(imidazole-$d_4$) complex of $(OEC)Fe^{III}$ [27] is fairly similar to that of the bis-4-$Me_2$NPy complex just discussed; the NMR spectra of this complex were discussed in the accompanying paper in comparison to those of the (oxo-OEC)-$Fe^{III}$ complex.[27] The $OECFe^{III}$ pyrroline-$CH_2$ shift is somewhat larger (17.9 ppm), while that of the 8,17-$CH_2$ resonances (26.1 ppm) and the spread of all resonances at 30 °C are

**Table 1.** Proton Chemical Shifts of 2,3-Pyrroline, 8,17-$CH_2$, and *meso* Protons of $[(OEC)Fe(L)_2]^+$ and $CH_2$ and *meso*-H Protons of $[OEP(L)_2]^{+a}$

| | chem shift, ppm | | | | | | | | |
|---|---|---|---|---|---|---|---|---|---|
| | $[(OEC)Fe(L)_2]^+$ | | | | | | | $[OEP(L)_2]^+$ | |
| ligand L | pyrroline-H | 8,17-$CH_2$ | 12,13-$CH_2$ | 7,18-$CH_2$ | 2,3-$CH_2$ | *meso*-5,20 | *meso*-10,15 | $CH_2$ | *meso*-H |
| imidazole | 12.0[a] | 37.0[a] | −0.4, 0.0[b] | 6.9, 7.1[b] | −5.0[b] | 8.3[b] | 3.4[b] | 5.3[a] | −1.4[a] |
| 4-(dimethylamino)pyridine | 17.8[a] | 41.5[a] | −2.8, −2.4[b] | 7.9, 8.4[b] | −6.8, −6.5[b] | 7.6[b] | 3.1[b] | 4.3[a] | NA[c] |
| pyridine | 29.2[a] | 55.0[a] | −0.8, −0.3[b] | 10.4, 10.7[b] | −6.6, −6.4[b] | 8.2[b] | 2.7[b] | 8.3[a] | NA[c] |
| 4-cyanopyridine | 51.3[a] | 64.8, 69.8[a] | NA[c] | NA[c] | −12.3, −11.5[a] | NA[c] | NA[c] | 14.2[a] | NA[c] |
| *tert*-butyl isocyanide | 128.3[a] | 40.3, 35.3[a] | NA[c] | 13.9, 14.5[b] | −4.9, −1.8[b] | −71.7[a] | −43.0[a] | 8.0[a] | −70[a,d] |

[a] Measured in $CD_2Cl_2$ at −60 °C (213 K). [b] Measured in $CD_2Cl_2$ at +30 °C (303 K). Temperature dependence of these resonances is very small. [c] NA = not assigned. [d] Taken from ref 62.

slightly smaller for the bis(imidazole) complex than they are for the bis-4-$Me_2$NPy complex shown in Figure 2a.

The chemical shift of the pyrroline-H of $[(OEC)Fe(Im\text{-}d_4)_2]^+$ at 303 K (+17.9 ppm) is somewhat smaller than those of bis(imidazole)iron(III) pyropheophorbide methyl ester at 298 K (~+24, +29.5 ppm),[19] while for other $(d_{xy})^2(d_{xz},d_{yz})^3$ ground-state chlorin complexes, $[(TPC)Fe(val\text{-}OMe)_2]CF_3SO_3$ and $[(TPC)Fe(PMe_2Ph)_2]CF_3SO_3$, the pyrroline protons are found at very positive chemical shifts, +57.3, 61.3,[26] and +64.6[24] ppm, respectively, both at 283 K. That the chemical shifts for the pyrroline-H should be positive (rather than negative) is supported by the fact that the pyrroline-H are attached to carbons that are not part of the $\pi$ system but are rather alkyl carbons attached to the α-carbons, which are part of the $\pi$ system of the chlorin ring; hence, the pyrroline-H of low-spin Fe(III) chlorins should always have positive chemical shifts,[36,37] based on this reasoning (however, see discussion of $[(TPC)Fe(t\text{-}BuNC)_2]^+$ below). The extremely positive chemical shifts of the two TPC complexes mentioned above, however, could suggest the possible involvement of a high- or intermediate-spin excited state in each of these latter cases, but the larger chemical shifts observed for these complexes than for the high-spin TPCFeCl[38] or OECFeCl (Figure 1) makes it clear that these mainly low-spin complexes have considerably more spin density at the α-carbons of the pyrroline ring than might have been expected on the basis of the bis(imidazole) complex of $(OEC)Fe^{III}$ and of the pyropheophorbide methyl ester Fe(III) complex.[19] The chemical shifts of the 8,17-$CH_2$ and pyrroline-H of all of the $(OEC)Fe^{III}$ complexes of this study at −60 °C are summarized in Table 1.

The lower basicity pyridine complexes of $(OEC)Fe^{III}$ show quite different behavior from those of $(TPC)Fe^{III}$,[38] $(TPP)Fe^{III}$,[39] and $(TMP)Fe^{III}$[40] complexes with the same axial ligands. With a decrease of the donor strength of the axial ligands, an increase instead of decrease[38,39−41] of the chemical shift of the pyrrole-8,17-$CH_2$ protons is observed, as shown in Figure 2b for the bis(pyridine-$d_5$) complex (assignments made on the basis of the spectra shown in Supporting Information Figures S3 and S4) and Figure 2c for the bis(4-cyanopyridine) complex (assignments made on the basis of the spectra shown in Figures S5 and S6). The behavior of the pyrroline protons is similar, and the order of the macrocycle chemical shifts for different axial ligands is a bit different, as summarized for the $^1$H chemical shifts at −60 °C in Table 1.

The NMR results suggest that, over the temperature range of the NMR studies, unlike low-spin $(TMP)Fe^{III}$[40,41] and $(TPC)Fe^{III}$[38] complexes, the low-basicity pyridine complexes of (OEC)Fe(III) do not change their ground state from $(d_{xy})^2(d_{xz}d_{yz})^3$ to $(d_{xz}d_{yz})^4(d_{xy})^1$ with a decrease of the donor strength ($pK_a(BH^+)$) of the axial ligands. If the larger positive $CH_2$ and pyrroline-H shifts were due to population of a low-spin $(d_{xy})^1(d_{xz},d_{yz})^4$ excited state, the *meso*-H resonances would shift to *negative* chemical shifts at higher temperatures. Rather, they remain in the diamagnetic region and are difficult to assign because of signal breadth and overlap at low temperatures; hence their shifts are presented at +30 °C in Table 1, and they do not change significantly as a function of temperature. The curved temperature dependence, Figure 4a,b, discussed below, is consistent with more intermediate- or high-spin character over the temperature range of the NMR measurements, as is the fact that the *meso*-H resonances remain in or close to the diamagnetic region throughout the temperature range investigated.

An intermediate-spin ground state has been found in some $\beta$-pyrrole alkyl-substituted porphyrins with weakly basic pyridine ligands (for example, $[(OEP)Fe(3\text{-}ClPy)_2]Cl$[42] and $[(OEP)Fe(3,5\text{-}Cl_2Py)_2]Cl$[43,44]). A study of the dependence of the solution magnetic moment (ranging from 2.0 to 4.4 $\mu_B$) of a large number of $[(P)Fe(3\text{-}ClPy)_2]ClO_4$ complexes indicated that species with more basic porphyrinate ligands (such as OEP) have higher spin multiplicity.[45] As a possible explanation, it was suggested that the more basic porphyrins donate more electron density to the $Fe^{III}$ ion and thus decrease its charge attraction for the axial ligands, which results in a decrease of the axial ligand field, leading to higher spin multiplicity.[45] Furthermore, NMR studies of the highly saddled octaethyltetraphenylporphyrin complex $[(OETPP)Fe(4\text{-}CNPy)_2]ClO_4$ showed that this complex has a $S = 3/2$ spin state,[46] while the less-saddled $[(OMTPP)Fe(4\text{-}CNPy)_2]ClO_4$ and $[(TC_6TPP)Fe(4\text{-}CNPy)_2]ClO_4$ complexes showed "intermediate" behavior, with $(d_{xz},d_{yz})^4(d_{xy})^1$ ground states at 4.2 K and $S = 3/2$ excited states over the temperature range of the solution NMR investigations.[46]

For comparison to these $(OEC)Fe^{III}$ complexes, the $(OEP)Fe^{III}$ complexes with different axial substituted pyridine

(42) Scheidt, W. R.; Geiger, D. K.; Hayes, R. G.; Lang, G. *J. Am. Chem. Soc*. **1983**, *105*, 2625−2632.
(43) Kintner, E. T.; Dawson, J. H. *Inorg. Chem*. **1991**, *30*, 4892−4897.
(44) Scheidt, W. R.; Osvath, S. R.; Lee, Y. J.; Reed, C. A.; Shavez, B.; Gupta, G. P. *Inorg. Chem*. **1989**, *28*, 1591−1595.
(45) Geiger, D. K.; Scheidt, W. R. *Inorg. Chem*. **1984**, *23*, 1970.
(46) Yatsunyk, L. A.; Walker, F. A. *Inorg. Chem*. **2004**, *43*, 757−777.

ligands were also studied by $^1$H NMR spectroscopy in this work. It was found that [(OEP)Fe(4-$Me_2$NPy)$_2$] $ClO_4$ has the smallest chemical shifts while [(OEP)Fe(4-CNPy)$_2$]$ClO_4$ has the largest over the temperature range of the NMR studies (303−183 K). The chemical shifts at −60 °C of the pyrrole-$CH_2$ resonances of the corresponding OEP complexes to those of the OEC complexes of this study are included in Table 1. For [(OEP)Fe(4-CNPy)$_2$]$ClO_4$ and [(OEP)Fe(Py)$_2$]-$ClO_4$, the chemical shifts of the pyrrole-$CH_2$ protons show anti-Curie behavior, indicating a change of the spin state with temperature and possibly chemical exchange between mono- and bis(ligand) complexes at the higher temperatures. With an increase in temperature, the chemical shifts have more contribution from the species with high- or intermediate-spin state, especially for [(OEP)Fe(4-CNPy)$_2$]$ClO_4$, leading to larger chemical shifts. However, NMR studies detailed enough to determine which higher spin state ($S = 3/2$ or $S = 5/2$) is involved were not carried out for these OEP complexes.

The temperature dependence experiments for the (OEC)-$Fe^{III}$ complexes (Figure 4a,b) show similar behavior, although the pyrrole-$CH_2$ shifts of the chlorin complexes show less strong anti-Curie behavior than the porphyrin analogues. The Curie plots of [(OEC)Fe(4-$Me_2$NPy)$_2$]Cl and [(OEC)Fe(Im-$d_4$)$_2$]Cl are almost straight lines, with intercepts approximately equal to the diamagnetic shift at $1/T = 0$. However, for [(OEC)Fe(4-CNPy)$_2$]$^+$ and [(OEC)Fe(Py-$d_5$)$_2$]$^+$, the Curie plots of both pyrrole-8,17-$CH_2$ and pyrroline protons are curved. With an increase in temperature, the plots bend upward, to more positive chemical shifts. This suggests that the observed pyrrole-$CH_2$ shifts have contributions from high- or intermediate-spin species, as in the case of the (OEP)$Fe^{III}$ complexes having the same ligands, discussed above. However, with the limited temperature-dependent chemical shift data obtained in this work, it is not possible to tell whether these species are involved in chemical equilibria with high- or intermediate-spin state species at room temperature or whether there is a thermally accessible excited state that is highly populated at elevated temperatures. The fact that the chemical shifts of the pyrrole-$CH_2$ and pyrroline-H resonances for the bis(pyridine) complex (Figure 2b) and the bis(4-cyanopyridine) complex (Figure 2c) are larger than those of the high-spin chloroiron(III) complex at 30 °C (Figure 1) and that the *meso*-H resonances have positive chemical shifts suggests that the excited state is 6-coordinate high-spin ($S = 5/2$), where the $a_{2u}(\pi)$-type interaction with the $d_{z^2}$ orbital pointed out by Cheng and coworkers[47] no longer contributes to the negative *meso*-H shifts observed in the 5-coordinate high-spin complex, and the $\beta$-pyrrole $CH_2$ shifts are increased by the increased $\sigma$-delocalization when the iron is in the mean plane of the macrocycle.[48]

**EPR Spectra.** Although the NMR studies have not fully defined the nature of the spin state changes over the temperature range 183−303 K, the EPR spectra, obtained in frozen $CD_2Cl_2$ solutions at 4.2 K and shown in Figure 5,

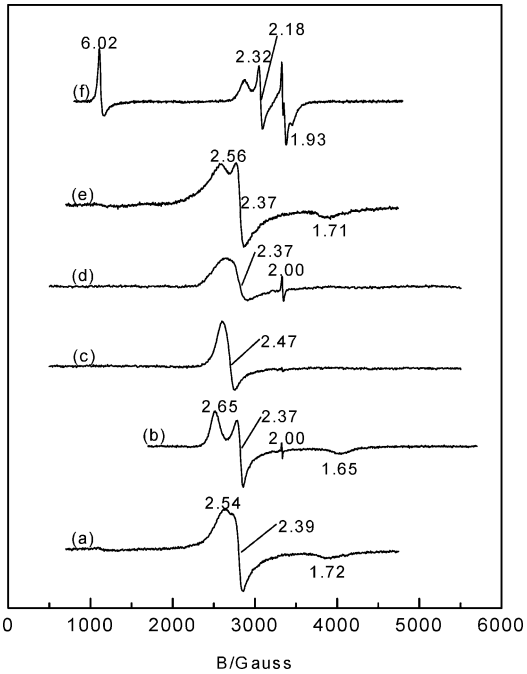


**Figure 5.** EPR spectra of (a) [(OEC)Fe(Im-$d_4$)$_2$]$^+$, (b) [(OEC)Fe(4-$Me_2$-NPy)$_2$]$^+$, (c) [(OEC)Fe(Py)$_2$]$^+$, (d) [(OEC)Fe(4-CNPy)$_2$]$^+$, (e) for comparison [(oxo-OEC)Fe(Im-$d_4$)$_2$]Cl,[27] and (f) [(OEC)Fe(*t*-BuNC)$_2$]$^+$. The signal with the *g* values of 6.02 and 2.00 in (f) comes from the high-spin impurity (OEP)FeCl; a free radical signal with $g = 2.03$ is also observed for this complex.

show that the ground state of all of these complexes is $S = 1/2$ and that, with a decrease in the donor strength of the axial ligands, the spectra of (OEC)$Fe^{III}$ complexes become more axial, with the largest *g*-value moving to smaller values as the basicity of the pyridine decreases. For the bis(pyridine) and bis(4-cyanopyridine) complexes, the smallest *g*-value is no longer resolved. All complexes have similar enough *g*-values that it is not possible to tell unequivocally, without pulsed EPR data,[49−51] whether there is a switch in ground state from $(d_{xy})^2(d_{xz},d_{yz})^3$ to $(d_{xz},d_{yz})^4(d_{xy})^1$ as the basicity of the pyridine ligands decreases. However, the apparent switch to axial symmetry for the bis(pyridine) and bis(4-cyanopyridine) complexes and the fact that the largest (and only resolved) *g*-value (2.47, 2.37, respectively, Figure 5) is smaller than that observed for [(TPP)Fe(4-CNPy)$_2$]$^+$ (2.62)[52] and [(TMP)Fe(4-CNPy)$_2$]$^+$ (2.53),[53] which has been shown by NMR,[53] EPR,[53] and MCD[54] spectroscopies to have the $(d_{xz},d_{yz})^4(d_{xy})^1$ ground state, strongly suggests this possibility.

(47) Cheng, R.-J.; Chen, P.-Y.; Lovell, T.; Liu, T.; Noodleman, L.; Case, D. A. *J. Am. Chem. Soc.* **2003**, *125*, 6774−6783.

(48) As shown in Figure 18 of ref 36, at 294 K the $CH_2$ resonances of OEPFeCl in $CD_2Cl_2$ occur as two peaks at 41.2 and 45 ppm, while the same resonance of the same complex at the same temperature in DMSO-$d_6$ (where two DMSO molecules have replaced the chloride anion on the axial positions) occurs as one peak at 46.4 ppm; thus, the average chemical shift is about 3.3 ppm larger in this 6-coordinate complex. The difference could be larger in the complexes of the present study.

(49) Raitsimring, A. M.; Borbat, P.; Shokhireva, T. Kh.; Walker, F. A. *J. Phys. Chem.* **1996**, *100*, 5235−5244.

(50) Schünemann, V.; Raitsimring, A. M.; Benda, R.; Trautwein, A. X.; Shokhireva, T. Kh.; Walker, F. A. *J. Biol. Inorg. Chem.* **1965**, *4*, 708−716.

(51) Astashkin, A. V.; Raitsimring, A. M.; Walker, F. A. *J. Am. Chem. Soc.* **2001**, *123*, 1905−1913.

(52) Safo, M. K.; Walker, F. A.; Raitsimring, A. M.; Walters, W. P.; Dolata, D. P.; Debrunner, P. G.; Scheidt, W. R. *J. Am. Chem. Soc.* **1994**, *116*, 7760−7770.

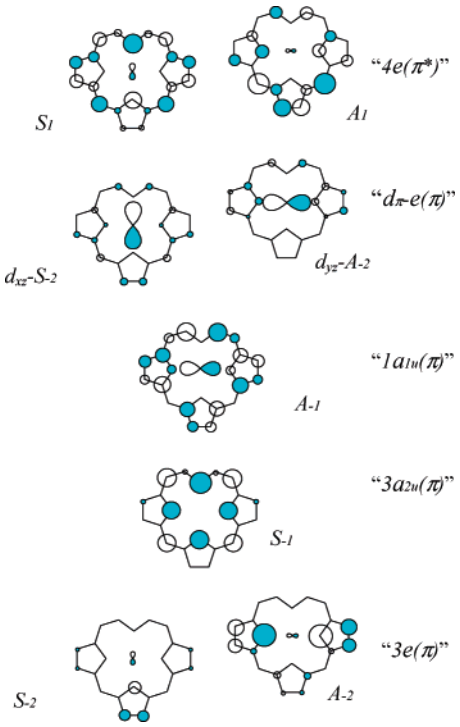


**Figure 6.** Hückel frontier orbitals of the chlorin ring for low-spin Fe(III) complexes with $(d_{xy})^2(d_{xz}d_{yz})^3$ ground state. The orbitals are placed vertically according to their approximate relative energies calculated using the program MPORPHw,[28] and the highest (singly) occupied orbital is the $d_{yz}$-$A_{-2}$. The sizes of the circles stand for the magnitudes of the electron density at each position; the expectation is that the electron density at each macrocycle position will be the same as the spin density at that position for orbitals that have proper symmetry to interact with the unpaired electron(s) of the metal. $A_{-2}$ and $S_{-2}$ are the antisymmetric and symmetric (with respect to the pseudo mirror plane that bisects the $C_2-C_3$ bond of the pyrroline ring and the $C_{12}-C_{13}$ bond of the opposite pyrrole ring) analogues of the 3e($\pi$) orbitals of the porphyrin ring, $S_{-1}$ is the analogue of the $3a_{2u}(\pi)$ orbital of the porphyrin ring, $A_{-1}$ is the analogue of the $1a_{1u}(\pi)$ orbital of the porphyrin ring, which for the chlorin has correct symmetry for interaction with one of the metal $d_\pi$ orbitals, $d_{yz}$-$A_{-2}$ and $d_{xz}$-$S_{-2}$ are the analogues of the $d_\pi$-3e($\pi$) orbitals of a metalloporphyrin, which are largely composed of the metal $d_\pi$ orbitals, and $A_1$ and $S_1$ are the analogues of the 4e($\pi$*) orbitals of the porphyrin ring. For each orbital, the approximate relative contribution of the chlorin $\pi$ and metal $d_\pi$ is indicated by the size of the constituent orbitals shown.

**Electronic Structure Calculations.** The order of the average chemical shifts of the three pyrrole-$CH_2$ doublets of the bis(imidazole)[27] and bis(4-dimethylaminopyridine) (Figure 2a) complexes of $OECFe^{III}$ is exactly the same as the order of the spin densities predicted from the character of the highest occupied molecular orbital, the antisymmetric $d_{yz}$-$A_{-2}$ orbital, obtained from Hückel calculations using the program MPORPHw[28] (Figure 6). For simplicity, the chlorin orbitals in Figure 6 are labeled antisymmetric (*A*) or symmetric (*S*) with respect to the mirror plane that is perpendicular to the chlorin plane and bisects the pyrroline and opposite pyrrole rings. In the $C_2$ point group of the molecule with the complete pyrroline ring, the orbitals labeled as antisymmetric transform as *a* symmetry and the orbitals labeled as symmetric transform as *b* symmetry. Hence, as for $[(OEP)Fe(HIm)_2]^+$ [36,55,56] and $[(OEP)Fe(4\text{-}Me_2\text{-}NPy)_2]^+$ (this work), the antisymmetric *3e(π)*-type orbital $A_{-2}$ as combined with the $d_{yz}$ orbital to create the $d_{yz}$-$A_{-2}$ orbital shown in Figure 6 appears to be the primary metal−macrocycle interaction that defines the chemical shifts in the high-basicity pyridine complex of $(OEC)Fe^{III}$.

The order of energies shown in Figure 6 is only slightly different for the DFT calculations on the $[(OMC)Fe(ImH)_2]$ molecule, as shown in Figure 7. Both the ADF and the GAUSSIAN calculations place the antisymmetric $d_{yz}$-$A_{-2}$ orbital as the highest occupied orbital. The five highest occupied orbitals are close in energy, and the partitioning of metal and macrocycle character in these orbitals is sensitive to the energy of the metal d orbitals relative to the chlorin orbitals. In the ADF calculation the metal d orbitals are relatively less stable and the highest occupied orbitals are thus dominated by metal character. In the GAUSSIAN calculation the metal d orbitals are more stable and the metal d and chlorin $\pi$ orbitals are heavily mixed; thus the $d_{yz}$ orbital appears to interact almost equally with the two antisymmetric chlorin orbitals $d_{yz}$-$A_{-2}$ and what we must call $d_{yz}$-$A_{-1}$ because of the heavy mixing, in the calculation for the bis(imidazole) complex shown in Figure 7. It is clear that the degree of interaction with one or the other can change significantly depending on the $\sigma$-donor/$\pi$-donor/$\pi$-acceptor properties of particular axial ligands. Stabilization of the metal orbitals favors increasing macrocycle character in the HOMO. This point will be emphasized in the comparison with the bis(isocyanide) complex discussed below. The spin density calculated for the $[(OMC)Fe(HIm)_2]^+$ cation by the ADF method is shown in Figure 8A, and the similarity to the character of the HOMO displayed in Figure 6 and Figure 7 is evident.

Because the chlorin ring was constrained to being planar in the calculations shown in Figure 7, the $S_{-1}$ and $d_{xy}$ orbitals cannot interact, although they would be expected to interact strongly if the chlorin ring were allowed to ruffle,[47,52] as shown in the calculated SOMO of the ruffled bis-*t*-BuNC complex, Figure 8C; in analogy to the structures of the bis(imidazole) or bis(4-dimethylaminopyridine) complexes of $OEPFe^{III}$,[57,58] we assume that if planar axial ligands are in parallel planes the macrocycle will not be ruffled. Furthermore, the large positive chemical shift of the pyrroline-H (17.9 and 15.5 ppm for the bis(imidazole)[27] and bis(4-dimethylaminopyridine) complexes, respectively, at room temperature) is consistent with the involvement of the $d_{yz}$ orbital, which has proper symmetry to interact with the $A_{-1}$ chlorin orbital (Figures 6, 7, and 8A) to lead to spin delocalization to the pyrroline-H; the higher energy of the latter chlorin orbital than the $d_{yz}$-$A_{-2}$ orbital should make this interaction highly favorable, and the $\sigma$-donor and

(53) Safo, M. K.; Gupta, G. P.; Watson, C. T.; Simonis, U.; Walker, F. A.; Scheidt, W. R. *J. Am. Chem. Soc.* **1992**, *114*, 7066−7075.
(54) Cheesman, M. R.; Walker, F. A. *J. Am. Chem. Soc.* **1996**, *118*, 7373−7380.
(55) Walker, F. A.; La Mar, G. N. *Ann. N. Y. Acad. Sci.* **1973**, *206*, 328−348.
(56) La Mar, G. N.; Walker, F. A. *J. Am. Chem. Soc.* **1973**, *95*, 1782−1790.
(57) Mylrajan, M.; Andersson, L. A.; Sun, J.; Loehr, T. M.; Thomas, C. A.; Sullivan, E. P., Jr.; Thomson, M. A.; Long, K. M.; Anderson, O. P.; Strauss, S. H. *Inorg. Chem.* **1995**, *34*, 3953−3963.
(58) Safo, M. K.; Gupta, G. P.; Walker, F. A.; Scheidt, W. R. *J. Am. Chem. Soc.* **1991**, *113*, 5497−5510.

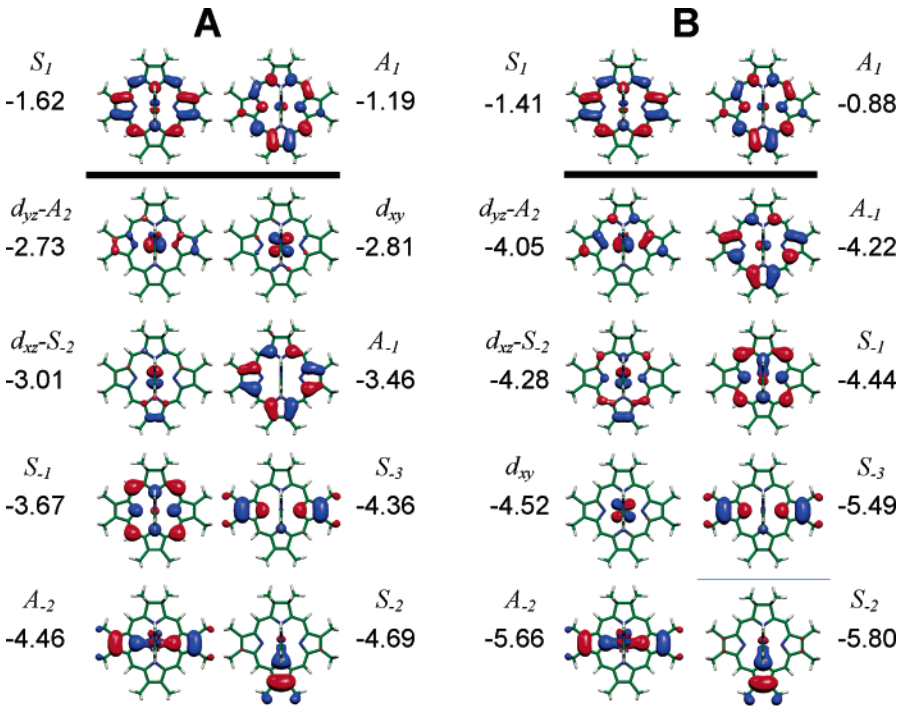


**Figure 7.** Molecular orbitals obtained from the (A) ADF and (B) GAUSSIAN calculations on the [(OMC)Fe(ImH)$_2$] molecule. The red and blue colors emphasize the symmetry properties of the orbitals. The names utilized for the Hückel orbitals shown in Figure 6 are applied to these orbitals as well, except that the $d_{xy}$ metal orbital was not shown in Figure 6 and the $S_{-3}$ orbital (which cannot interact with the d-orbitals) is not shown in Figure 6 because the Hückel calculation places it at lower energy than those of the $S_{-2}$ and $A_{-2}$ orbitals. The $d_{xy}$ orbital cannot interact in the chosen geometry (planar chlorin ring) but is expected to interact with the $S_{-1}$ orbital if the chlorin ring is ruffled. In the $C_2$ point group of the molecule with the complete pyrroline ring, the orbitals labeled as antisymmetric transform as a symmetry and the orbitals labeled as symmetric, along with the $d_{xy}$ orbital, transform as b symmetry.

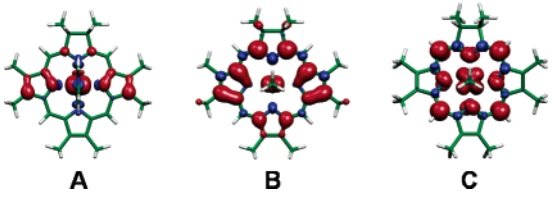


**Figure 8.** Calculated spin densities by the ADF method for (A) [(OMC)-Fe(ImH)$_2$]$^+$ in the planar geometry, (B) [(OMC)Fe(MeNC)$_2$]$^+$ in the planar geometry, and (C) [(OMC)Fe(MeNC)$_2$]$^+$ in the ruffled geometry. The red and blue colors represent positive and negative spin density, respectively.

$\pi$-donor/acceptor characteristics of particular axial ligands can be expected to modulate this interaction, thus leading to very different pyrroline-H chemical shifts for different axial ligand complexes. Hence, as for [(OEP)Fe(HIm)$_2$]$^+$ [59−61] and [(OEC)Fe(4-Me$_2$NPy)$_2$]$^+$ (this work), the antisymmetric *3e-(π)*-type orbital $A_{-2}$ as combined with the $d_{yz}$ orbital to create the $d_{yz}$-$A_{-2}$ orbital shown in Figures 6 and 7 appears to be primarily involved in the metal−macrocycle interactions in this higher-basicity pyridine complex, with additional contribution from the $A_{-1}$ orbital.

As for the lower basicity pyridine complexes whose large positive NMR shifts were discussed above, the ADF calculations for the bis(imidazole) complex place the α-spin metal $d_{z^2}$ orbital (the LUMO) only about 1.5 eV higher in energy than the HOMO, and the $d_{x^2-y^2}$ orbital is only 0.5 eV higher than that; both of these would be even closer in energy to the HOMO for the lower basicity pyridines. Hence, either a $S = 3/2$ or $S = 5/2$ state may be populated at NMR temperatures; however, an equally acceptable interpretation of the increasingly positive chemical shifts and curved temperature dependences of the bis(pyridine) and -(4-cyanopyridine) complexes would be that the $S_1$ chlorin orbital, which is calculated to lie at an energy between those of the $d_{z^2}$ and $d_{x^2-y^2}$ orbitals, may also be involved in spin delocalization at NMR temperatures; this orbital has relatively large density at the 7,18 and 8,17 pyrrole carbons, the pyrroline-α-carbons, and the *meso*-carbons. The effects of different donor abilities of the axial ligands on the orbital and spin density characters is illustrated by Figure 7A,B, which compare the calculated characters of the $d_{yz}$-$A_{-2}$ orbitals obtained with different stabilities of the metal d orbitals relative to the chlorin orbitals, and by Figure 8A,B, which compare the calculated spin densities of the bis-(imidazole) and "flat" bis(isocyanide) complexes. The stronger axial donors (Figures 7A and 8A) lead to the smaller $CH_2$ chemical shifts because of the increased metal character and decreased macrocycle character in the SOMO.

**[(OEC)Fe(*t*-BuNC)$_2$]$^+$.** The NMR spectrum of [(OEC)-Fe(*t*-BuNC)$_2$]$^+$ is quite different in some respects from those of the imidazole and pyridine complexes of (OEC)Fe$^{III}$. Figure 9 shows the $^1$H spectrum of [(OEC)Fe(*t*-BuNC)$_2$]CF$_3$-SO$_3$ in $CD_2Cl_2$ at 30 °C. It is characterized by a strongly downfield, very broad peak at 132 ppm (pyrroline-H) and two upfield peaks at −15 (*meso*-10,15-H) and −30 ppm (*meso*-5,20-H). The rest of the spectrum is similar in pattern

(59) Walker, F. A.; La Mar, G. N. *Ann. N. Y. Acad. Sci.* **1973**, *206*, 328−348.
(60) La Mar, G. N.; Walker, F. A. In *The Porphyrins*; Dolphin, D., Ed.; Academic Press: New York, 1979; Vol. IV, pp 61−157.
(61) La Mar, G. N.; Walker, F. A. *J. Am. Chem. Soc.* **1973**, *95*, 1782−1790.

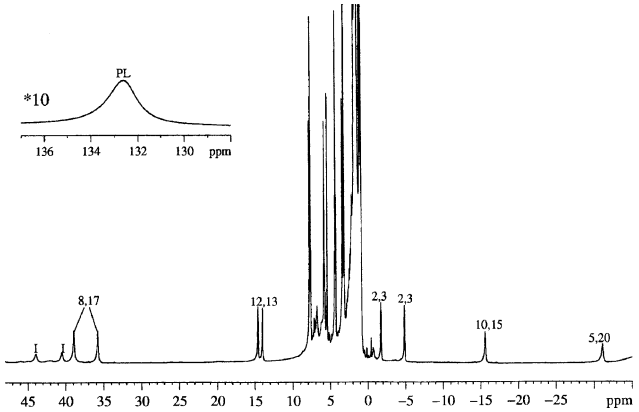


**Figure 9.** $^1$H spectrum of $[(OEC)Fe(t\text{-}BuNC)_2]^+$ in $CD_2Cl_2$ at 25 °C. I = impurity, the high-spin (OEP)FeCl produced by oxidation of (OEC)FeCl and incomplete replacement of chloride by trifluoromethylsulfonate. The numbers indicate the positions of the $CH_2$ groups and *meso* protons. Insert: Pyrroline proton signal (the vertical scale is increased 10-fold).

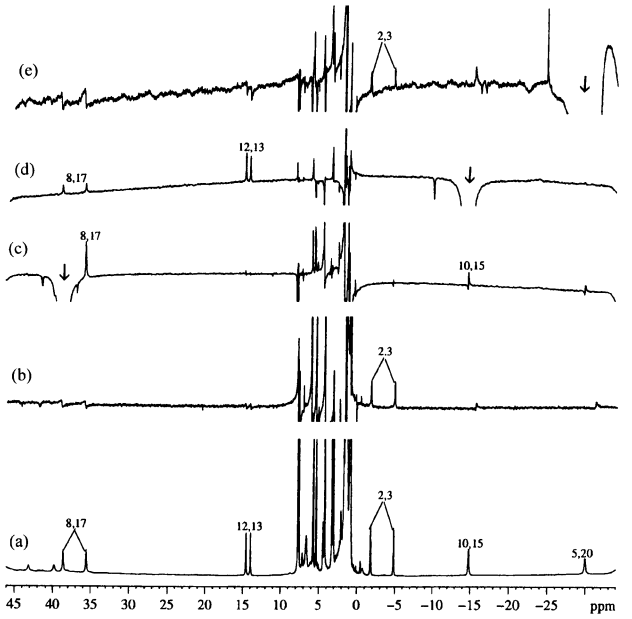


**Figure 10.** NOE difference spectra of $[(OEC)Fe(t\text{-}BuNC)_2]^+$ in $CD_2Cl_2$ at 30 °C. (a) is the control spectrum; the others are difference spectra. The arrow in (c)−(e) indicates the position of irradiation in each case. In (b), the pyrroline proton peak is irradiated (at 132 ppm).

and chemical shifts to those of the bis(pyridine) and -imidazole complexes of $(OEC)Fe^{III}$. The chemical shift of the *tert*-butyl group of the bound ligand is uncertain because this peak is located in the diamagnetic region and not resolved. The full assignments of the ethyl and *meso* protons were made from COSY (Figure S7) and NOE difference experiments (Figure 10). In the COSY spectrum, cross-peaks between the two inequivalent $CH_2$ protons and between the $CH_2$ and the $CH_3$ protons within each ethyl group were observed. Included in the COSY spectrum are the correlations of the 7,18-$CH_2$ protons with each other and their methyl group, which are all found in the crowded diamagnetic region at 4.5, 3.3, and 2.5 ppm, respectively (Supporting Information Figure S7). However, the peak of the pyrroline-H is so broad that no cross-peak between the pyrroline protons and the pyrroline-2,3-$CH_2$ group is detectable in the COSY spectrum. The pyrroline protons were assigned from NOE difference

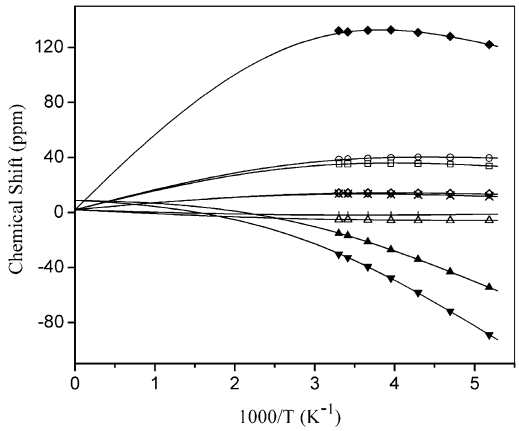


**Figure 11.** Curie plot of $[(OEC)Fe(t\text{-}BuNC)_2]^+$: ◆, pyrroline protons; ▲, ▼, *meso* protons; ○, □, ◇, ×, +, △, pyrrole-$CH_2$ protons. Solid lines are the fits obtained using the TDFw program,[76] with energy separation between ground and excited state $E_{21} = 467$ cm$^{-1}$ and the spin densities $\rho_1$ and $\rho_2$ given in Table 2.

experiments. The difference spectrum of Figure 10b shows that when the peak of the pyrroline-H (at 132 ppm) was irradiated, the NOE from the pyrroline-2,3-$CH_2$ was detected. Other assignments were made in the same way as were those for the bis(pyridine) (this work) and bis(imidazole)[27] complexes of $(OEC)Fe^{III}$. The Curie plots of these peaks are shown in Figure 11. The temperature dependence of all resonances is far from that expected for Curie behavior, except for those resonances with small chemical shifts.

Although the chemical shifts of the three doublets from the pyrrole-$CH_2$ groups of $[(OEC)Fe(t\text{-}BuNC)_2]^+$ are similar to those of the corresponding Im-$d_4$[27] and 4-$Me_2$NPy (Figure 2a) complexes, there are two unique features for $[(OEC)Fe(t\text{-}BuNC)_2]^+$: (i) The pyrroline protons have a very large positive chemical shift (of opposite sign and much larger in magnitude than the pyrroline-H of $[(TPC)Fe(t\text{-}BuNC)_2]^+$ [25]), consistent with the spin density distribution in Figure 8B, calculated assuming a flat chlorin ring, thus indicating that the OEC ring system behaves quite differently than the TPC ring system. (ii) The resonances of the *meso* protons are shifted far upfield to −15.5 and −31 ppm at 298 K. In the low-spin $[(OEP)Fe(t\text{-}BuNC)_2]^+$ complex, which has the $(d_{xz}d_{yz})^4(d_{xy})^1$ ground state, the *meso* protons also show negative chemical shifts (−37 ppm at 303 K).[62]

In analogy to the $[(OEP)Fe(t\text{-}BuNC)_2]^+$ complex, the large $\pi$ spin density at the *meso* positions of the corresponding OEC complex may be due to spin delocalization involving macrocycle → Fe $\pi$ donation from the $S_{-1}$, $3a_{2u}(\pi)$-type orbital of the ruffled macrocyclic ring to the singly occupied $d_{xy}$ orbital of the metal center.[63−66] Indeed, a number of

(62) Walker, F. A.; Nasri, H.; Turowska-Tyrk, I.; Mohanrao, K.; Watson, C. T.; Shokhirev, N. V.; Debrunner, P. G.; Scheidt, W. R. *J. Am. Chem. Soc.* **1996**, *118*, 12109−12118.
(63) For iron porphyrinates, the $a_{1u}(\pi)$ orbital does not have proper symmetry to interact with the $d_{xz}$ or $d_{yz}$ orbitals, but because of the lower symmetry of the macrocycle, the $A_{-1}$ orbital of iron chlorins does have proper symmetry to interact with the $d_{yz}$ orbital of low-spin Fe(III), as already pointed out by La Mar and co-workers.[64,65]
(64) Licoccia, S.; Chatfield, M. J.; LaMar, G. N.; Smith, K. M.; Mansfield, K. E.; Anderson, R. R. *J. Am. Chem. Soc.* **1989**, *111*, 6087−6093.
(65) Chatfield, M. J.; LaMar, G. N.; Parker, W. O.; Smith, K. M.; Leung, H.-K.; Morris, I. K. *J. Am. Chem. Soc.* **1988**, *110*, 6352−6358.

crystal structures of metallochlorinates have shown an increased tendency of the macrocycle to ruffle[67−74] than for the corresponding metalloporphyrinates. The ADF calculations on the low-spin $d^6$ [(OMC)Fe(MeNC)$_2$] complex show that, in comparison to the bis(imidazole) complex, the $d_{xz}$ and $d_{yz}$ orbitals are stabilized relative to the $d_{xy}$ orbital due to the $\pi$-accepting ability of the isocyanide and the $d_{xy}$ orbital thus becomes the HOMO of the complex. In the calculation of [(OMC)Fe(MeNC)$_2$]$^+$ as a planar gas-phase cation, the positive charge stabilizes the metal orbitals and the d orbital order reverts to that of the bis(imidazole) complex giving the similar calculated spin density shown in Figure 8B. However, the ADF calculations on the ruffled conformation of [(OMC)Fe(MeNC)$_2$]$^+$ show the creation of a sufficiently strong interaction between the $S_{-1}$ orbital and the $d_{xy}$ orbital that the resulting molecular orbital that represents donation of an electron from the $S_{-1}$ orbital to the $d_{xy}$ is the SOMO and results in the calculated spin density in Figure 8C. And while this interaction alone would indicate that both types of *meso*-H should have approximately the same chemical shift, rapid interchange between the planar and ruffled conformations, for which the spin densities are shown in Figure 8B,C, respectively, could explain different chemical shifts for the 5,20 and 10,15 *meso*-H. An equilibrium between the planar and ruffled chlorin ring also explains the sizable chemical shifts of the pyrrole-$CH_2$ protons, which are very small in [(OEP)Fe(*t*-BuNC)$_2$]$^+$.[62]

The spin density distribution on the chlorin ring of [(OEC)-Fe(*t*-BuNC)$_2$]$^+$ in the ground and first excited states can be obtained from the Curie plot of Figure 11 using the two-level temperature dependence fitting program, TDFw.[75,76] Pseudocontact shifts were considered part of the contact shifts in this fitting procedure because both have inverse temperature dependence; the Curie factor used for the *meso*-H (−496.8 ppm K$^{-1}$) was opposite in sign and different in magnitude than that for $CH_2$ groups and the pyrroline-H (+591.4 ppm K$^{-1}$),[36,37,77] as should be the case for the opposite-sign isotropic shifts expected for protons directly bound to the aromatic carbon of the macrocycle and those one aliphatic bond removed therefrom.[36,37] The most consistent fit was found to be that for which the ground state has $S = 1/2$ with a mixed $(d_{xz},d_{yz})^4(d_{xy})^1$ and $(d_{xy})^2(d_{xz},d_{yz})^3$ electron configuration (probably an equilibrium between the two, as discussed in the previous paragraph) and the first excited state has $S = 5/2$, with calculated separation between the ground and excited state of 467 cm$^{-1}$, or about $2.2kT$ at room temperature. The calculated spin densities on positions 8,17, 12,13, and 2,3, the *meso* positions and positions 1,4 (where the pyrroline saturated carbons and their methylene protons are attached) in the ground state ($\rho_1$) and excited state ($\rho_2$), obtained from the fit shown in Figure 10, are given in Table 2.

**Table 2.** Spin Densities Obtained from the Temperature-Dependent Fit of the $^1$H NMR Resonances[75,76] (Figure 10) on Positions of Interest in the Ground State (1) and the First Excited State (2) of [(OEC)Fe(*t*-BuNC)$_2$]$^+$

| posn | $\rho_1$ | $\rho_2$ |
|---|---|---|
| 1,4 | 0.0154 | 0.1054 |
| 2,3 | −0.0002 | −0.0033 |
| | −0.0015 | −0.0051 |
| av | −0.0009 | −0.0042 |
| 8,17 | 0.0068 | 0.0279 |
| | 0.0046 | 0.0267 |
| av | 0.0057 | 0.0273 |
| 12,13 | 0.0016 | 0.0099 |
| | 0.0008 | 0.0100 |
| av | 0.0012 | 0.0100 |
| 10,15 | 0.0336 | −0.0004 |
| 5,20 | 0.0508 | 0.0023 |

As can be seen, for the ground state, there are large spin densities at the four *meso* positions and smaller spin densities at pyrrole-8,17 (and yet smaller at the other pyrrole positions, with the sign of the spin density at the 2,3-$CH_2$ being negative because the pseudocontact contribution was included as part of the contact shift in this calculation) but much larger at the 1,4 carbons. This spin density distribution is qualitatively consistent with that predicted for the $S_{-1}$ orbital (Figure 6) but is more consistent with the average of the $d_{yz}$-$A_{-2}$ and $d_{xy}$-$S_{-1}$ SOMO orbitals of a flat and a ruffled chlorin ring, Figure 8B,C. This average would strongly suggest a rapid (on the NMR time scale) equilibrium between the two electronic ground states, with their very different spin density distributions. In support of this, the frequency of the ruffled-planar vibration of [(OMC)Fe(MeNC)$_2$], obtained from the DFT calculations, is found to be 22 cm$^{-1}$, an extremely low frequency.

It is interesting to note that the sign and magnitude of the spin density at the *meso*-carbons is predicted to be fairly small and *negative* for the flat chlorin ring, Figure 8B, in which the metal orbital involved is $d_{yz}$, but quite large and *positive* for the ruffled chlorin ring, Figure 8C, in which the metal orbital involved is $d_{xy}$, while the sign of the spin density at the 1,4-carbons is predicted to be large and positive for the flat chlorin ring but smaller and negative for the ruffled chlorin ring. Although the average of the *meso*-C spin densities is not in quantitative agreement with that observed for [OECFe(t-BuNC)$_2$]$^+$ (larger negative chemical shift for the *meso*-5,20-H and smaller negative chemical shift for the *meso*-10,15 positions, indicating larger positive spin density

(66) The $3a_{2u}(\pi)$ orbital in a planar porphyrin ring does not have proper symmetry to interact with any d orbital of the metal; it can interact with the metal $d_{xy}$ orbital if the porphyrin ring is strongly ruffled.[52,62]

(67) Stolzenberg, A. M.; Stershic, M. T. *Inorg. Chem.* **1987**, *26*, 1970−1977.
(68) Andersson, L. A.; Loehr, T. M.; Stershic, M. T.; Stolzenberg, A. M. *Inorg. Chem.* **1990**, *29*, 2278−2285.
(69) Renner, M. W.; Furenlid, L. R.; Barkigia, K. M.; Forman, A.; Shim, H.-K.; Simpson, D. J.; Smith, K. M.; Fajer, J. *J. Am. Chem. Soc.* **1991**, *113*, 6891−6898.
(70) Senge, M. O.*J. Photochem. Photobiol., B: Biol.* **1992**, *16*, 3−36.
(71) Connick, P. A.; Haller, K. J.; Macor, K. A. *Inorg. Chem.* **1993**, *32*, 3256−3264.
(72) Senge, M. O.; Ruhlandt-Senge, K.; Smith, K. M. *Z. Naturforsch.* **1995**, *50b*, 139−146.
(73) Senge, M. O.; Ruhlandt-Senge, K.; Lee, S.-J. H.; Smith, K. M. *Z. Naturforsch.* **1995**, *50b*, 969−981.
(74) Ozawa, S.; Watanabe, Y.; Morishima, I. *Tetrahedron Lett.* **1994**, *35*, 4141−4144.
(75) Shokhirev, N. V.; Walker, F. A. *J. Phys.Chem.* **1995**, *99*, 17795−17804.
(76) TDFw is a two-level data fitting program for processing of the temperature dependence of the NMR shifts of paramagnetic complexes, developed by Dr. Nikolai V. Shokhirev.[75] See: http://www.shokhirev.com/nikolai/programs/prgsciedu.html.
(77) Banci, L.; Bertini, I.; Luchinat, C.; Pierattelli, R.; Shokhirev, N. V.; Walker, F. A. *J. Am. Chem. Soc.* **1998**, *120*, 8472−8479.

at the 5,20-meso-carbons), it is likely that the calculated spin densities for both ring conformations will be sensitive to a number of factors that might reverse the order of *meso*-H shifts.

The large positive pyrroline-H chemical shift of [OECFe(t-BuNC)$_2$]$^+$ (+132 ppm at 298 K, Figure 9) indicates major importance of the flat chlorin ring conformation in producing an average of large positive spin density at the 1,4-carbons. In comparison, the pyrroline-H chemical shift of [(TPC)Fe(*t*-BuNC)$_2$]$^+$ is −36 ppm at 298 K.[25] As mentioned above, from a simple point of view the pyrroline-H chemical shift should not be negative in low-spin Fe(III) chlorinates of either electronic ground state because they are protons attached to an aliphatic carbon, for which the predicted chemical shift is positive.[36,37,78] Hence, a negative chemical shift for the pyrroline-H of [(TPC)Fe(*t*-BuNC)$_2$]$^+$ is indicative of *negative* spin density at the α-carbons of the pyrroline ring of this $S = 1/2$ complex[78] and, thus, a noninnocent chlorin macrocycle. Because the bis(isocyanide) complexes of *meso*-phenyl-substituted porphyrins[62,79] (and undoubtedly chlorins) are more ruffled than are those of *β*-pyrrole-substituted porphyrins[62] (and undoubtedly chlorins), it is possible that [(TPC)Fe(*t*-BuNC)$_2$]$^+$ does not participate in an equilibrium between ruffled and planar ring conformations as discussed with respect to the OEC analogue, and thus it has negative spin density at the 1,4-carbons, as shown in Figure 8C.

For the excited state of [OECFe(*t*-BuNC)$_2$]$^+$, there is very large spin density at the pyrroline position (Table 2), indicating that the $A_{-1}$ orbital of the chlorin ring (Figures 6, 7) or the $d_{xy}$-$S_{-1}$ SOMO of a ruffled chlorin ring (Figure 8C) plays an important role in the spin delocalization of the $S = 5/2$ excited state or that the $S_1$ chlorin orbital contributes to the large spin density of the excited state. The two-level fitting program predicts negligible spin density on the 10,15-*meso* positions in the excited state but small positive spin density on the 5,20-*meso* positions. This is consistent with the fact that the high-spin complex should be 6-coordinate, thus eliminating the possible involvement of delocalization via the $d_{z^2}$ metal orbital,[47] discussed below.

A $(d_{xz}d_{yz})^4(d_{xy})^1$ ground state for [OECFe(*t*-BuNC)$_2$]$^+$ is strongly supported by the EPR spectrum, Figure 9f, which, although it is rhombic (three *g*-values, 2.32, 2.18, 1.93; $g_\perp = 2.25$, $g_\parallel = 1.93$), has very small differences between the *g*-values and a small $\Sigma g^2 = 13.86$, both of which are very similar to the EPR parameters of [(OEP)Fe(*t*-BuNC)$_2$]$^+$ and [(TPP)Fe(*t*-BuNC)$_2$]$^+$ ($g_\perp = 2.28$, 2.21, $g_\parallel = 1.83$, 1.93, $\Sigma g^2 = 13.74$, 13.49, respectively),[62] and thus suggest that it also very likely has a $(d_{xz}d_{yz})^4(d_{xy})^1$ ground state, at least at 4.2 K where the EPR spectrum was recorded.

**High-Spin (OEC)FeCl.** With two chiral carbons, *trans*-(OEC)FeCl has two enantiomers that are mirror images of each other, Chart 1. These two enantiomers have exactly the same NMR spectrum, and thus it is not necessary (and would not be possible) to separate them. The $^1$H spectrum (Figure 1) of high-spin *trans*-(OEC)FeCl has been reported, and the assignments of the *meso* protons have been made by selective deuteration.[80] Unlike its bis(ligand) complexes, (OEC)FeCl does not have $C_2$ symmetry. Thus, there should be a total of 16 different $CH_2$ resonances (12 from pyrrole-$CH_2$ groups and 4 from the pyrroline-$CH_2$ group) from the eight ethyl groups, two different pyrroline protons, and four different *meso* protons. Thus, the claim of slow or no interconversion between supposed ruffled conformations of *trans*-(OEC)-FeCl,[74] as evidenced by the presence of four *meso*-H signals, relied on the misconception that the 5,20 and 10,15 *meso*-H could interconvert via ring inversion of the macrocycle when in a nonplanar conformation. In contrast, the observation of only two *meso*-H signals for (*cis*-3,4-dihydroxyoctaethylchlorinato)iron(III) chloride at room temperature, which split into four resonances at low temperatures,[74] is indeed indicative of macrocycle inversion of this nonplanar chlorin.

Although the types of protons of (OEC)FeCl were assigned previously,[80] the full assignment of the eight ethyl groups has not previously been reported. In this study, we report the full resonance assignments for high-spin (OEC)FeCl, as summarized in Figure 1, obtained using saturation transfer (ST) techniques. To conduct the ST experiments, an NMR sample containing a mixture of (OEC)FeCl and its low-spin complex, [(OEC)Fe(4-Me$_2$NPy)$_2$]Cl, was made by adding less axial ligand to the solution of (OEC)FeCl than necessary to fully form the bis(ligand) complex (4-Me$_2$NPy:(OEC)-FeCl ≈ 1:1). Only the $^1$H NMR resonances of (OEC)FeCl and [(OEC)Fe(4-Me$_2$NPy)$_2$]$^+$ were observed in this sample, and thus no mono(ligand) complex was present, due to its relative instability, which clearly causes it to disproportionate to the HS chloride and LS bis(ligand) complexes. The saturation transfer experiments were carried out on this mixture. Irradiation of the pyrrole-$CH_2$ peaks of the high-spin (OEC)FeCl form and observation of the saturation transfer to the corresponding peaks of the low-spin species, already assigned as described above that arise from chemical exchange between the two, when recorded as a difference spectrum, allow the peaks of (OEC)FeCl to be assigned. Similar procedures have been utilized to assign the heme resonances of the HS Fe(III) form of Nitrophorin 2, where 1-MeIm was used as the ligand to form the low-spin complex whose $^1$H NMR spectrum had been assigned previously by COSY and NOESY techniques.[81,82] The control spectrum (Figure S8a) shows the assignments derived for all the $CH_2$ groups and pyrroline protons from the experiments shown in Figure S8b-o, except for two peaks from the pyrroline-2,3-$CH_2$ protons, which are under or very close to the envelope of resonances of the low-spin [(OEC)Fe(4-Me$_2$-NPy)$_2$]Cl. Figure 12 shows the saturation transfer experiments that led to the assignments of the four *meso* protons,

(78) Walker, F. A. *Inorg. Chem*. **2003**, *42*, 4526−4544.
(79) Simonneaux, G.; Schünemann, V.; Morice, C.; Carel, L.; Toupet, L.; Winkler, H.; Trautwein, A. X.;Walker, F. A. *J. Am. Chem. Soc*. **2000**, *122*, 4366−4377.
(80) Sullivan, E. P., Jr.; Grantham, J.; Thomas, C. S.; Strauss, S. H. *J. Am. Chem. Soc*. **1991**, *113*, 5264−5270.
(81) Shokhireva, T. Kh.; Shokhirev, N. V.; Walker, F. A. *Biochemistry* **2003**, *42*, 679−693.
(82) Shokhireva, T. Kh.; Berry, R. E.; Uno, E.; Balfour, C. A.; Zhang, H.; Walker, F. A. *Proc. Natl. Acad. Sci. U.S.A.* **2003**, *100*, 3778−3783.

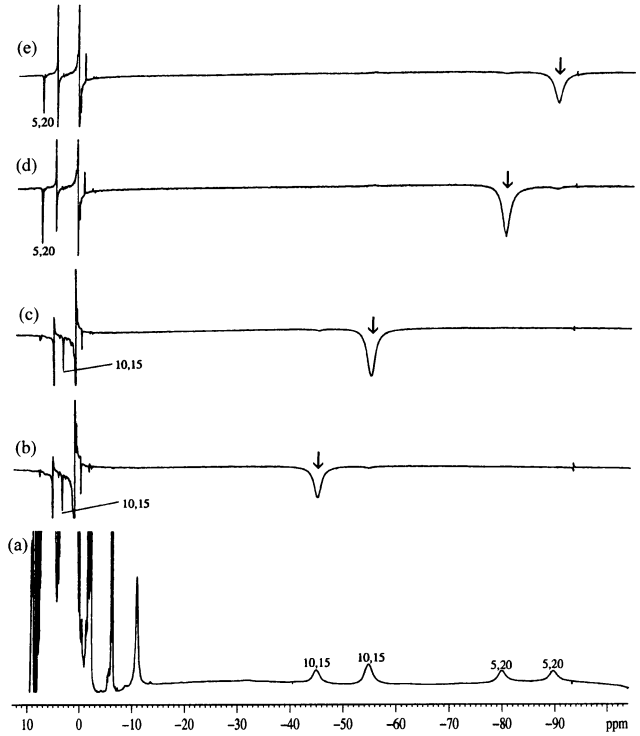


**Figure 12.** Saturation transfer experiment for the *meso*-protons of the mixture of [(OEC)Fe(4-$Me_2$NPy)$_2$]Cl and (OEC)FeCl obtained at 30 °C in $CD_2Cl_2$. (a) is the control spectrum; the others are difference spectra. The arrows show the positions of irradiation in each experiment.

which are consistent with the assignments in the literature obtained by selective deuteration of the chlorin ring.[80]

An interesting finding in the saturation transfer experiments is that when any resonance from one of the pyrrole-$CH_2$ groups is irradiated, besides the chemical exchange signal from the corresponding low-spin species, there is another negative-phase signal observed from the high-spin (OEC)FeCl. This ST resonance is from the chemical exchange between two $CH_2$ protons in two different but symmetry-related (such as positions 12,13 or 7,18 or 8,17) ethyl groups. This chemical exchange arises from the binding, loss, and rebinding of chloride ion on the opposite side of the chlorin ring in the process of exchange with the 4-$Me_2$NPy ligands. For example, for one of the two $CH_2$ protons at position 8, if the chloride ion leaves when 4-$Me_2$NPy binds, a different $Cl^-$ can bind to the metal center on the opposite side when 4-$Me_2$NPy leaves, and this proton will thereby have its chemical environment changed to that of a $CH_2$ proton at position 17 by virtue of the enantiomeric relationship shown in Chart 1. This process only occurs in the mixture of (OEC)FeCl and [(OEC)Fe(4-$Me_2$NPy)$_2$]Cl. (1-MeIm and HIm bind too tightly and exchange too slowly to produce saturation transfer signals, while pyridine and 4-CNPy do not bind tightly enough and exchange too rapidly to allow resolved high-spin resonances to be observed.) As a result, chemical exchange signals were observed between two symmetry-related $CH_2$ groups. This chemical exchange was also observed in the NOESY/EXSY spectrum (Figure S9) of the mixture of (OEC)FeCl and [(OEC)Fe(4-$Me_2$NPy)$_2$]-Cl. Since there are a total of 10 pyrrole-$CH_2$ peaks in the paramagnetically shifted region from 36 to 56 ppm, 5 pairs of cross-peaks should be and are observed (the 2,3-$CH_2$ resonances are not present in this spectral region).

**Table 3.** $^1$H NMR Shifts of (OEC)FeCl[a]

| chem shift, ppm | av shift, ppm | assgnt |
|---|---|---|
| 56.5, 51.0, 48.3, 42.4 | 49.6 | 12,13-$CH_2$ |
| 51.5, 51.0, 46.1, 45.1 | 48.4 | 8,17-$CH_2$ |
| 39.3, 38.4, 37.9, 35.3 | 37.7 | 7,18-$CH_2$ |
| 26.0, 19.5, 15.0, 10.3 | 17.7 | 2,3-$CH_2$ |
| 28.8, 24.7 | 26.8 | 2,3-PL |
| −47, −57 | −52 | 10,15-*meso* |
| −84, −94 | −89 | 5,20-*meso* |
| 39, 43[b] | 41[b] | $CH_2$ of (OEP)FeCl[b] |
| −56[b] | −56[b] | *meso*-H of (OEP)FeCl[b] |

[a] Recorded in $CD_2Cl_2$ at 30 °C. [b] Recorded in $CDCl_3$ at 29 °C.[36]

Interestingly, in the NOESY/EXSY spectrum, only chemical exchange between the $CH_2$ protons of the high-spin (OEC)FeCl is observed. Chemical exchange between (OEC)-FeCl and [(OEC)Fe(4-$Me_2$NPy)$_2$]Cl was not observed in the NOESY/EXSY spectrum due to the large difference of the relaxation rates of these two species. Thus, it is clear that if one wants to observe the chemical exchange or NOE between a rapidly and a slowly relaxing resonance, the steady-state experiment is a much better choice than the NOESY/EXSY experiment. By irradiating the rapidly relaxing peak and observing the change of the slowly relaxing peak, one can avoid the disadvantage of the NOESY experiment, the decrease of the signal during the $t_1$ increment and mixing time due to the fast relaxation rate of the fast-relaxing species.

Pawlik et al.[14] have compared the isotropic shifts of high-spin (OEP)FeCl, (OEC)FeCl, (TPP)FeCl, and (TPC)FeCl and studied the spin delocalization on the chlorin ring in detail, despite the fact that the pyrrole-H and pyrrole-$CH_2$ peaks were not individually assigned. They found that, for (TPC)-FeCl, two pyrrole-H resonances are at lower frequency and one is at higher frequency than the pyrrole-H resonance for the (TPP)FeCl, while for (OEC)FeCl and (OEP)FeCl the mirror image of this pattern is observed: two sets of four pyrrole-$CH_2$ resonances are at higher chemical shift and one set of four is at lower chemical shift than the average pyrrole-$CH_2$ resonances for (OEP)FeCl. They thus concluded that, in both (TPC)FeCl and (OEC)FeCl, the $\sigma$ contributions to the contact shifts of the pyrrole-H or pyrrole-$CH_2$ protons are the same for the three kinds of positions and that the difference in the isotropic shifts arises from the different $\pi$ delocalization contributions to the three kinds of positions. Our assignments, summarized in Table 3, also show that two average pyrrole-$CH_2$ resonances of (OEC)FeCl are at higher chemical shift and one average pyrrole-$CH_2$ resonance is at lower chemical shift than the average pyrrole-$CH_2$ resonance of (OEP)FeCl. However, the pattern of (OEC)FeCl is not the mirror image of (TPC)FeCl; the average shift of OEC pyrrole-7,18-$CH_2$ protons is the smallest (and the shift of the TPC pyrrole-7,18-H is the largest), but the average shift of OEC pyrrole-8,17-$CH_2$ is smaller than that of pyrrole-12,13-$CH_2$, while the shift of pyrrole-8,17-H is also smaller than the shift of pyrrole-12,13-H in (TPC)FeCl.[38] Two possible factors may contribute to this difference in behavior of the two chlorins: (i) Each $CH_2$ group has a different $\theta$ angle (the angle between the C−C−H plane and the $p_\pi$ axis

of the chlorin ring), leading to the fact that the $\pi$ contact shift of a pyrrole-$CH_2$ group is not directly proportional to the spin density on the pyrrole position to which it is attached.[83] (ii) The different dipolar shifts of the lower symmetry chlorin ring may also play a role in determining the chemical shifts of pyrrole-$CH_2$ protons.

As in (OEP)FeCl, the contact shifts of the *meso* protons of (OEC)FeCl have contributions from both $\sigma$ and $\pi$ spin delocalization.[9] The *meso*-5,20 protons have larger negative isotropic shifts and, hence, larger $\pi$ spin densities (assuming the contributions from the dipolar shift and $\sigma$ spin distribution are the same for the two kinds of *meso* positions) than the *meso*-10,15 protons, suggesting that the $A_1$ orbital (Figures 6 and 7, one of the analogues of the $4e(\pi^*)$ orbitals of the porphyrin) is not involved in this $\pi$ spin delocalization, as was earlier thought to be the case for (OEP)FeCl and (TPP)FeCl.[36,37,84] Rather, the pattern of spin delocalization to the *meso* positions is most consistent with that expected for the filled orbital $S_{-1}$, Figures 6 and 7. It has been shown recently that, for a five-coordinate metallomacrocyclic complex in which the metal is markedly out of the plane of the four nitrogens of the macrocycle, an unpaired electron in the $d_{z^2}$ orbital of the metal can interact with the $a_{2u}$-type $\pi$ orbital of the macrocycle to cause large $\pi$ spin delocalization to the *meso*-carbons[47] and that this is the major contribution to the large negative chemical shifts of the *meso*-H of chloroiron(III) OEP and other porphyrins,[47] as well as the OEC of this study.

## Conclusions

Complexes $[(OEC)Fe(L)_2]^+$ (L = Im-$d_4$,[27] 4-$Me_2$NPy) are low-spin Fe(III) species. The EPR spectra at 4.2 K suggest that, with a decrease of the donor strength of the axial ligands, the complexes change their ground state from $(d_{xy})^2(d_{xz}d_{yz})^3$ to $(d_{xz}d_{yz})^4(d_{xy})^1$. The NMR data from 303 to 183 K show that the chemical shifts of pyrrole-8,17 protons increase with a decrease in the donor strength of the axial ligands (Py, 4-CNPy). This difference probably comes from the presence of partial high- or intermediate-spin species in the solution when the axial ligands are not sufficiently strong donors, and a contributing factor is the increasing macrocycle character of the SOMO as the metal orbitals become more stable with weaker axial donors. From 303 to 183 K, the $(d_{xy})^2(d_{xz}d_{yz})^3$ state still dominates the spin delocalization mechanism to the chlorin ring for the bis-4-$Me_2$NPy (this work) and -Im-$d_4$[27] complexes. The full peak assignments of the $[(OEC)Fe(L)_2]^+$ complexes of this study have been made from COSY and NOE difference experiments. The pyrrole-8,17-$CH_2$ and pyrroline protons show large chemical shifts (hence indicating large $\pi$ spin density on the adjacent carbons which are part of the $\pi$ system), while pyrrole-12,13-$CH_2$ and -7,18-$CH_2$ protons show much smaller chemical shifts. This order is consistent with the results from the corresponding $(TPC)Fe^{III}$ complexes[38] and the spin densities obtained from molecular orbital calculations.

For $[(OEC)Fe(t\text{-}BuNC)_2]^+$, the chemical shift pattern of the pyrrole-$CH_2$ protons looks somewhat like the pattern for $[(OEC)Fe(4\text{-}Me_2NPy)_2]^+$ or $[(OEC)Fe(Im\text{-}d_4)_2]^+$,[27] while the chemical shifts of the *meso* protons are similar to those of $[(OEP)Fe(t\text{-}BuNC)_2]^+$.[62] The chlorin ring of $[(OEC)Fe(t\text{-}BuNC)_2]^+$ appears to be in rapid equilibrium between planar and ruffled conformations. $[(OEC)Fe(t\text{-}BuNC)_2]^+$ has the $(d_{xz}d_{yz})^4(d_{xy})^1$ ground state at 4.2 K but appears to have a mixed $(d_{xz}d_{yz})^4(d_{xy})^1$ and $(d_{xy})^2(d_{xz},d_{yz})^3$ electron configuration over the temperature range of the NMR studies, with a high-spin ($S = 5/2$) excited state lying at somewhat more than $2kT$ at room temperature above the averaged orbital ground state. The pattern of spin delocalization at ambient temperatures appears to be the average of that expected for the *a*-symmetry SOMO of a flat chlorin ring (Figure 8B) and the *b*-symmetry SOMO of a ruffled chlorin ring (Figure 8C) that are in rapid equilibrium.

Proton resonance assignments for the high-spin (OEC)FeCl have been made by saturation transfer techniques that depend on chemical exchange between the HS chloride and LS bis-4-$Me_2$NPy complexes. The contact shifts of the pyrrole-$CH_2$ protons depend on both $\sigma$ and $\pi$ spin delocalization. The contact shifts of the *meso* protons of (OEC)FeCl also have two contributions, one from $\sigma$ (positive shift) and one from $\pi$ (negative shift) spin delocalization. The *meso*-5,20 protons have a larger negative chemical shift than the *meso*-10,15 protons, suggesting that the antibonding $A_1$ orbital (Figure 6) is not involved in the $\pi$ spin delocalization. Rather, the pattern of spin delocalization to the *meso* positions is most consistent with that expected for a combination of the filled $S_{-1}$ and $A_{-1}$ orbitals (Figures 6 and 7). By analogy, the orbital involved in the negative shift of the *meso*-H of (OEP)FeCl is the $3a_{2u}(\pi)$, which can interact with the $d_{z^2}$ orbital of the metal in these 5-coordinate high-spin chloroiron(III) complexes.[47]

**Acknowledgment.** The National Institutes of Health, Grant DK-31038 (F.A.W.), and National Science Foundation, Grant CHE0416004 (D.L.L.) and Grant CHE9610374 to the University of Arizona Molecular Structure Laboratory, are gratefully acknowledged. This paper was written while F.A.W. was a Visiting Professor and Alexander von Humboldt Senior Awardee in Science in the Physics Institute of the University of Lübeck. She thanks Professor Alfred X. Trautwein for his hospitality and friendship.

**Supporting Information Available:** Figures S1−S9, showing spectra. This material is available free of charge via the Internet at http://pubs.acs.org.

IC0490876

(83) La Mar, G. N., Horrocks, W. D., Jr., Holm, R. H., Eds. *NMR of Paramagnetic Molecules*; Academic Press: New York, 1973.
(84) La Mar, G. N.; Eaton, G. R.; Holm, R. H.; Walker, F. A. *J. Am. Chem. Soc.* **1973**, *95*, 63−75.